POLYTECHNIQUE MONTRÉAL

affiliée à l'Université de Montréal

Efficacy of Paper Sensors for the Detection and Quantification of Nitric Oxide

SYED HASSAN ALI

Institut de génie biomédical

Mémoire présenté en vue de l'obtention du diplôme de *Maîtrise ès sciences appliquées*

Génie biomédical

Juin 2024

POLYTECHNIQUE MONTRÉAL

affiliée à l'Université de Montréal

Ce mémoire intitulé :

Efficacy of Paper Sensors for the Detection and Quantification of Nitric Oxide

présenté par **Syed Hassan ALI**

en vue de l'obtention du diplôme de *Maîtrise ès sciences appliquées*

a été dûment accepté par le jury d'examen constitué de :

Gregory DE CRESCENZO, président
Raphaël TROUILLON, membre et directeur de recherche
Lucien WEISS, membre

ACKNOWLEDGEMENTS

The author would like to acknowledge the support provided by the Bioanalytical Systems Laboratory (BASyL) and its members. Specifically, the author would like to acknowledge the supervision and support provided by Professor Raphaël Trouillon throughout this research project. I would also like to thank my family for the support provided throughout this research project.

RÉSUMÉ

Les capteurs d'oxyde nitrique (NO) à base de papier sont des dispositifs combinant les avantages des capteurs en papier aux méthodes électrochimiques pour la détection et la quantification du NO en temps réel. Le NO est un médiateur biologique d'importance en raison de son rôle dans diverses maladies, dont le cancer. Dans cet article, des capteurs en papier recouverts de Nafion et d'eugénol électropolymérisé sont utilisés pour détecter et mesurer le NO. La sensibilité, la limite de détection et le taux de production et de dégradation du NO sont calculés pour déterminer l'utilité de ces capteurs dans les environnements biologiques. En outre, la sélectivité de ces capteurs vis-à-vis du NO par rapport à d'autres composés biologiques est également mesurée en comparant la réponse des capteurs en présence d'autres molécules. La sensibilité médiane des capteurs en papier était de 488,3 (366,8-776,9) $\mu AM^{-1}mm^{-2}$ et les capteurs avaient une limite de détection médiane de 1,7 (1,4-2,3) µM. Des données préliminaires de mesure en culture cellulaire ont été obtenues, confirmant la possibilité d’utiliser ces capteurs pour des analyses biologiques quantitatives. Les capteurs sont sensibles et sélectifs, ce qui en fait une option intéressante pour la recherche biomédicale et la détection. Les recherches futures devraient examiner comment améliorer la limite de détection et la sélectivité des capteurs.

ABSTRACT

Nitric oxide (NO) is a mediator molecule of biological significance because of its role in various maladies including cancer. Paper-based NO sensors are devices that utilize the benefits of paper sensors and electrochemical methods for the detection and quantification of NO in real-time. In this paper, Nafion coated and electropolymerized eugenol paper sensors are utilized to determine the relationship between NO concentration and current. The sensitivity, limit of detection (LOD), and the rate of production and degradation of NO is calculated to determine the utility of these sensors in biological environments. As well, the selectivity of these sensors to NO compared to other biological compounds is also measured by calculating the comparative response of the sensors in the presence of other molecules. The median sensitivity of the paper sensors was 488.3 (366.8-776.9) $A*M^{-1}mm^{-2}$ and the sensors had a median LOD of 1.7 (1.4-2.3) µM. The sensors are also highly selective to NO with the sensors capturing a relatively much lower response from other biological molecules that could potentially interfere with the signal. Preliminary data were acquired in cell culture, showing the possibility for using these sensors for quantitative biological analysis. The sensors are sensitive and selective which makes them an attractive option for biomedical research and detection. Future research should examine how to lower the LOD further and improve the selectivity of the sensors.

TABLE OF CONTENTS

LIST OF TABLES

LIST OF FIGURES

LISTE OF SYMBOLS AND ABBREVIATIONS

3D Three-dimensional

ATP Adenosine triphosphate

CE Counter electrode

cGMP Cyclic guanosine monophosphate

CHD Coronary heart disease

CNS Central nervous system

CNT Carbon nanotubes

CV Cyclic voltammetry

DAF Diaminofluoresceins

DAN Diaminonaphthalene

DPV Differential pulse voltammetry

EC Endothelial cells

ECM Extracellular matrix

EDRF Endothelium derived relaxing factor

ePAD Electrochemical paper analytical device

EPC Endothelial progenitor cell

EPR Electron paramagnetic resonance

ESR Electron spin resonance

ETC Electron transport chain

EUG Eugenol

GC Guanylate cyclase

HUVEC Human umbilical vein-derived endothelial cell

KCl Potassium Chloride

LOD Limit of detection

MRI Magnetic resonance imaging

MW Molecular weight

NADPH Nicotinamide-adenine dinucleotide phosphate oxidase

NaOH Sodium hydroxide

NO Nitric oxide

NOS Nitric oxide synthase

eNOS Endothelial nitric oxide synthase

iNOS Induced nitric oxide synthase

MRI Magnetic resonance imaging

MRS Magnetic resonance spectroscopy

mtNOS Mitochondrial nitric oxide synthase

nNOS Neuronal nitric oxide synthase

O_2 Oxygen gas

ODE Ordinary differential equation

PAD Paper analytical device

PBS Phosphate buffer solution

PDMS Polydimethylsiloxane

PNS Peripheral nervous system

RE Reference electrode

Redox Reduction-oxidation

ROS Reactive oxygen species

RNS Reactive nitrogen species

SEM Scanning electron microscopy

VEGF Vascular endothelial growth factor

WE Working electrode

WPB Weibel-Palade bodies

XPS X-ray photoelectron spectroscopy

LIST OF APPENDICES

CHAPTER 1 INTRODUCTION

1.1 Context and Objectives of Study

Cancer is one of the major causes of death worldwide. It is the leading or second leading cause of death in over 100 countries in individuals under the age of 70[1]. In 2020, there were nearly 20 million new cases of cancer and approximately 10 million deaths worldwide. The burden of cancer on global public health is expected to rise with projections of over 28 million new cases in 2040. This projected rise of 47% in the annual number of cancer cases is a consequence of aging and growing populations worldwide and could potentially be intensified by an increase in other cancer risk factors[1].

It is therefore of critical importance to study further the chemical and biological makeup of cancer as well as develop and ameliorate methods of cancer detection and treatment. There are currently a variety of methods available for cancer detection. These diagnostic techniques include a physical examination of the patient as well as test conducted upon the blood or urine of a patient. Detection methods also include medical imaging techniques such as positron emission tomography (PET), X-ray computed tomography (CT), magnetic resonance imaging (MRI), and magnetic resonance spectroscopy (MRS). Furthermore, there are also molecular diagnostic methods ranging from liquid biopsy to flow cytometry[2]. Early detection can be a matter of critical importance as it has been demonstrated to improve the prognosis of the disease because of the higher efficacy of treatment at early stages. One of the consequences to many forms of cancer treatment are the adverse effects on non-cancerous tissues and cells or the rest of the body [3].

This underlines the significance of differentiation between cancerous and non-cancerous or healthy cells and tissues. One difference between healthy and cancerous cells is that cancerous cells are associated with nitric oxide (NO) secretion at significantly higher rates than healthy cells [4]. Therefore, the detection and quantification of the concentration of NO secretion in cell culture can provide insight into the presence of cancer as well as efficacy of various treatment methods.

This study addresses the use of paper sensors for the detection of NO utilizing electrochemical methods in endothelial cell culture. The methodology for the fabrication of NO sensors is adapted from the study titled *Detection of Nitric Oxide Release from Single Neurons in the Pond Snail,*

Lymnaea Stagnalis by Patel et al in 2006 [5]. The study by Patel et al utilized carbon fiber microelectrodes and this study will focus on the benefits of using paper electrodes as NO sensors.

The objective of this study is to fabricate NO sensors on paper and characterize their properties such as sensitivity, selectivity, and detection limit. This will be done using electrochemical techniques and the relationship between current and NO concentration will be determined. Finally, this study will also utilize the sensors in endothelial cell culture.

1.2 Thesis Outline

The outline of this study is as follows. There are eight chapters followed by references and appendices. Chapter One is an introduction providing the necessary context for this study and the objectives it seeks to fulfill. Chapter Two is a literature review analyzing the current field of study regarding nitric oxide (NO), electrochemical detection methods, paper sensors, and cell culture. Chapter Three further expands on the specific objectives of this research and the solutions it proposes to achieve these objectives. Chapter Four outlines the methodology employed by this study to achieve the objectives. Chapter Five and Chapter Six are two scientific articles produced from the research conducted in this study. Chapter Seven discusses the general results and implications of this study. Chapter Eight is composed of conclusions that can be drawn from the research conducted for this study and recommendations for future studies.

CHAPTER 2 LITERATURE REVIEW

This chapter will examine the existing literature regarding the main foci of this research. It will examine nitric oxide (NO) from a molecular, historical, and physiological perspective. It will examine various methods to detect NO, specifically electrochemical methods, and detail their advantages and drawbacks. Subsequently, this review will analyze the historical development of paper sensors as well as their various forms and uses. Finally, this review will examine the use of paper sensors in endothelial cell culture and the difficulties associated with the detection of NO in *in vitro* cell culture.

2.1 Nitric Oxide

2.1.1 History, Synthesis, and Molecular Overview

Nitric oxide (NO) is a ubiquitous biological molecule released by a variety of cells and performs a wide range of functions. NO was first discovered in the late eighteenth century by British chemist Joseph Priestley. It is a colorless toxic gas, and it is one of the most extensively studied molecules. Professor Salvador Moncada discovered the secretion of NO by endothelial cells [6]. The Nobel Prize in Physiology or Medicine was awarded to Ferid Murad, Robert F. Furchgott, and Louis J. Ignarro for the discovery of the role of NO as a signaling molecule in the cardiovascular system in 1998 [7]. The function of NO as an endothelium derived relaxing factor (EDRF) was reported in a 1987 paper by Ignarro et al [8]. According to Levin et al. in 2012, it is best known for its role in the vasculature [9].

The synthesis of NO is a product of several reduction-oxidation (redox) reactions with L-arginine, nicotinamide-adenine dinucleotide phosphate oxidase (NADPH), molecular oxygen, and NO synthases (NOS) enzymes. In this reaction, NO is formed *via* a reaction with L-arginine and NADPH in the presence of O_2 which degrades L-arginine to L-citrulline. NO is produced by different NOS in various tissues.

$$L-Arginine + NADPH + O_2 \xrightarrow{\substack{eNOS \\ iNOS \\ nNOS}} L-Citrulline + H_2O + NADP + NO$$

Figure 2-1: Chemical equation for the formation of NO via the degradation of L-arginine to L-citrulline in the presence of NOS enzymes.

There are three main types of NOS enzymes specifically, neuronal-NOS-1 (nNOS), inducible NOS-2 (iNOS), endothelial NOS-3 (eNOS). There are also some authors who refer to a fourth NOS enzymes called mitochondrial NOS (mtNOS). The NOS enzymes are produced by different tissues and bodily systems with nNOS being produced by neuronal and skeletal muscle tissue whereas the endothelium is where eNOS is primarily expressed. However, unlike the other NOS enzymes (nNOS and eNOS), iNOS is regulated at the level of gene transcription and is inducible in response to biological condition such as inflammation [9], [10], [11].

NO has a simple structure and a low molecular weight (MW) of 30.01 grams per mole, a density of 1.34 grams per litre, and a low solubility in water of 1.9 mM. NO is a free radical with an unpaired electron and therefore it is a very reactive molecule with a short half-life of 3-5 seconds *in vivo*, and it can only travel a limited distance before the molecule is oxidized [12]. These characteristics limit the bioavailability of NO temporally and spatially and increase the difficulty of detecting the molecule and quantifying its concentration [9].

2.1.2 Functions of NO

As stated above, there are various functions carried out by NO. It plays key roles in different bodily systems including the immune and nervous systems. NO that is derived from mtNOS has enormous impacts on the life and the death of cells. It 'effectively controls mitochondrial respiration, oxygen (O_2) consumption, transmembrane proton gradient and potential and adenosine triphosphate (ATP) synthesis'[9]. There are both acute and chronic impacts of NO on mitochondrial respiration. Inflammatory iNOS induction produces elevated NO levels which contest with O_2 causing a form of hypoxia referred to as "nitroxia" which produces reactive oxygen and nitrogen species (ROS/RNS). NO or RNS can permanently inhibit mitochondrial electron transport chain (ETC) complexes which undermines adenosine triphosphate (ATP) production which has cytotoxic effects. Therefore, acutely NO causes the reduction of mitochondrial oxidative metabolism. However, chronically it increases oxidative metabolism on a cellular level[13]. This is because it controls the content of the mitochondria and the energy balance of the body in response to the environment or internal bodily conditions and therefore functions as a "trigger" for the process of mitochondrial genesis. The seeming contradiction between nitric oxide causing a rise in oxidative metabolism on a cellular level while simultaneously decreasing the oxidative metabolism within

an individual mitochondrion in a cell is explained by the increase in mitochondrial efficiency[14]. Mitochondrial ETC produces adequate ATP and decreases consumption of oxygen.

NO plays a role in both cell protection and cell death. This is because it can instigate ‘adaptive cell survival signaling’ as it impacts mitochondrial defense mechanism which provides protection for the cells[15]. However, it also plays a role in cellular death as high NO concentration are cytotoxic. It can cause tyrosine nitration of cell elements, specifically of parts of the mitochondria and therefore play a central role in apoptosis. Extremely high amounts of NO can also result in mitochondrial failure through inhibiting the necessary respiration for cell survival[16]. This would prevent apoptosis and lead to necrosis because of an inability of the cells to acquire the energy essential for their survival.

There are three pathways by which NO carries out its role as a signaling molecule[17], [18]. The first mechanism involves activating guanylate cyclase (GC). The second mechanism involves the formation of S-nitroso thiol. The third mechanism involves the activation of mitogen protein kinases which is activated by the formation of peroxynitrite, a product of a reaction between NO and oxygen gas.

Furthermore, NO carries out a variety of functions in the central nervous system (CNS) and the peripheral nervous system (PNS). These functions range from modulating synaptic plasticity and the sleep-wake cycle to maintaining fluid balances and reproductive processes [19]. NO also has an impact on brain development, memory formation, and behaviour. The inhibition of NO produces amnesia which can be overcome through the injection of L-arginine [20]. NO inhibition also impairs spatial learning and olfactory memory [21]. Physiological amounts of NO are neuroprotective, however if NO is produced in excess it can cause cell damage and neurodegenerative diseases [22], [23].

As well, in the immune system NO plays many roles regarding infectious diseases, autoimmune processes, and chronic degenerative diseases. NO in the immune system is released by macrophages, among other cells, in response to cytokines and microbial compounds with anti-tumour and antimicrobial impacts [24]. In infectious diseases, NO can play a role in combatting the disease as it does in regards to malaria [25]. It can also exacerbate the illness, as is the case with HIV, likely because of the inhibition of T cell proliferation [26].

2.1.3 Function of NO in the Vasculature

As previously mentioned, one of the most famous aspects of NO is the significance of the molecule in the vasculature. Palmer *et al* first reported the release of NO by the vascular endothelium in 1987 [27]. In 1988, they discovered that NO was produced from L-arginine through the chemical reaction depicted in Figure 2-1[28]. NO controls blood flow and NO plays a significant role in the repair of the vasculature and angiogenesis[29]. The depletion of NO is correlated with a significant increase in blood pressure. It also regulates the oxygen consumption of the vessel wall. As a result, a decline in the availability of NO leads to blood circulation having a heightened sensitivity to available oxygen [30].

Endothelial cells generate vascular NO from eNOS. The endothelium is subjected to stress from external circumstances as well as chemical conditions and blood flow. One of the roles of NO is to protect the "functional ability" of endothelial progenitor cells (EPCs) to allow these cells to partake in the process of repairing the vasculature as well as angiogenesis [9]. Endothelial cells generate NO in response to hemodynamic stimuli and as a response to shear stress [31]. The NO can diffuse to smooth muscle cells where is activates soluble GC producing 3,5- cyclic guanosine monophosphate (cGMP) [32]. The activation of soluble GC invokes the first NO signaling mechanism discussed in the previous subsection and the production of cGMP is shown to mediate relaxation of smooth muscle cells. NO thus plays a role as a vasodilator. This has been demonstrated by the fact that NO inhibition using analogues of arginine in *in vitro* and *in vivo* prevents endothelium dependent relaxation of human vessels [33]. The most significant impact of NO inhibition on vasodilation is on vascular resistance. The resistance to blood flow almost doubles with the inhibition of NO and systemic NO inhibition elevates blood pressure [34]. In addition, hypertension has also been observed in mice in which lack the gene for eNOS illustrating the role of NO in mediating basal vasodilation [35].

NO also inhibits activation and expression of adhesion molecules in the vasculature. This prevents platelet aggregation and platelet adhesion to the endothelial surface contributing to its anti-inflammatory properties on the vessel wall [36]. NO also inhibits smooth muscle cell replication and migration [37], [38]. Furthermore, endothelial NO limits intimal hyperplasia after balloon injury [39].

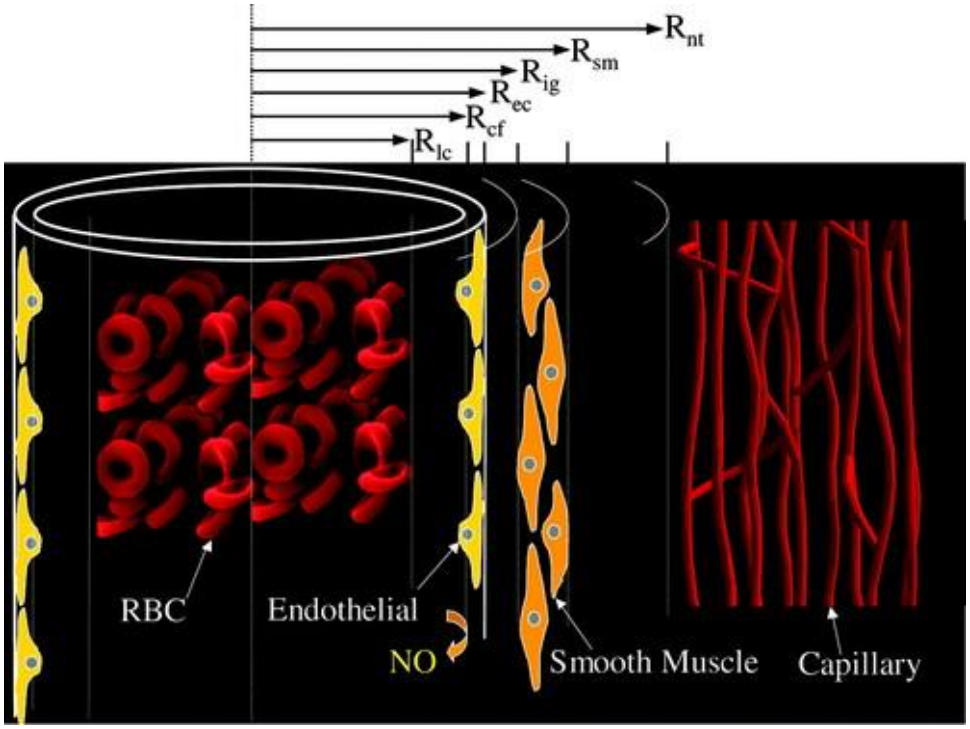

Figure 2-2: NO in the Endothelium. Reproduced with permission[32].

2.1.4 Bioavailability of NO in the Vasculature

There are various factors that could cause a reduction of the bioactivity and bioavailability of NO. The factors that impact the bioavailability of NO include decreased eNOS expression and activity, low levels of physical activity, and cell senescence[40]. Decreased eNOS expression may occur due to advanced coronary heart disease (CHD) which has a deleterious effect on NO production. The production of NO can also be lowered due to arginases because of the hydrolysis of L-Arginine. Low levels of physical activity would cause a reduction in eNOS expression because of the lower levels of blood flow and therefore NO production. Furthermore, low activity levels are associated low amount of shear stress. This has an adverse impact on NO production because fluid shear stress is one of the major factors in the production of NO. This is because NO production will allow the blood vessels to maintain homeostasis by returning the shear stress levels towards normal. Older cells also reduce NO levels because these cells are insulin resistant, and insulin promotes the production of NO under normal conditions[41].

There are a variety of physiological impacts of the low bioavailability of NO. The health impacts include abnormal vascular function, abnormal muscle metabolism, and insulin resistance. The

reduction of bioavailable NO results in the restriction of blood vessel (vasoconstriction) and inflammation[42]. Vasoconstriction will occur because a decline of NO bioavailability lead to a loss of vasodilators which serve to expand the blood vessels. Furthermore, prolonged chronically low levels of NO will lead to the thickening of the medial vessel wall and the stiffness of the vessel which is known as atherosclerosis[43]. Another impact of low levels of NO would be impaired muscle metabolism. This is because a decline in NO production would reduce the size of the mitochondria which would limit ATP production and oxygen consumption. As well, insulin resistance, which was previously mentioned as a potential cause of a decline in NO production, is also a consequence of low levels of NO which are correlated with the development of insulin resistance. This has been demonstrated in mice with mice that are deficient in eNOS suffering from insulin resistance.

2.2 Detection of NO

There are various methods of NO detection including colorimetric assays and fluorescent markers as well as chemiluminescence, electrochemistry, gas chromatography, and electron paramagnetic resonance (EPR) [12]. There are a variety of challenges in the detection of NO and improving the sensitivity and selectivity while lowering the limit of detection (LOD) remains challenging. The detection of NO *in vivo* is a difficult task because of the short half-life of 3-5 seconds in biological tissues as well as the fact that as a radical molecule it can freely react with other molecules [12], [44]. This is because of its radical nature which leads it to be quickly oxidized. As a result, direct measurements of NO *in vivo* are difficult to acquire and often NO is measured indirectly by studying its products such as nitrite and nitrate. Furthermore, recent research has suggested that the *in vivo* concentration range of NO is approximately 0.1-5 nM which is significantly lower than earlier studies has suggested [45]. However, the half-life in aqueous solutions is much longer (~500 seconds), which makes the *in vitro* detection of NO less challenging.

2.2.1 Colorimetry

The use of colorimetry for the detection of NO relies on the quantification of the colour change. The change in colour is the consequence of the two-step Griess reaction between nitrite and sulfanilic acid which produces a red-violet coloured dye which has a absorption peak of approximately 540 nm[46]. The reaction was first studied by the German chemist Johann Peter Griess in the late nineteenth century. The Griess assay is method for the indirect measurement of

NO through the measurement of nitrite. Colorimetry is a rapid and low-cost method that allows for the detection of NO. Furthermore, modifications to Griess assay can improve the resolution and efficiency of the technique [47]. However, it is an indirect method with low sensitivity and does not allow for localized measurements[48].

2.2.2 Fluorescence

Fluorescent markers are another method for NO detection with 2,3-diaminonaphthalene (DAN) and diaminofluoresceins (DAF) working as two common fluorescent agents [12]. DAN is a fluorescent agent that reacts quickly with N_2O_3 which is a product of a two-step reaction between two molecules of NO and oxygen [49]. The reaction between DAN and N_2O_3 produces 2,3-naphthotriazol (NAT) which is highly fluorescent with an excitation wavelength of 375 nm and an emission wavelength of 415 nm. The intensity of the fluorescence is proportional to the concentration of NO. Furthermore, NO as well as nitrite and nitrate do not directly react with DAN and therefore, the NO detection process will not interfere with the biological functions of the molecule. In addition, DAN has a limit of detection (LOD) of 10 nmol/L. However, there are problems associated with the use of DAN assays for NO detection, specifically its cytotoxicity and poor solubility in neutral buffer solutions. As well, the excitation wavelength for the fluorescent product is in the UV range (375nm) and UV light is damaging to cells. The requirement of UV light for excitation can also cause autofluorescence in a cellular sample. This interferes with the detection of NO by the fluorescent agent.

DAFs are another type of fluorescent agent used for the detection of NO. The fluorescent product emerges from the reactivity of amine groups with NO in the presence of O_2 [50]. The exact reaction mechanism is unknown; however, it is understood that DAF does not react with NO directly or with nitrate or nitrite. This allows for measurements which do not interfere with physiological functions of NO. Furthermore, DAFs have an excitation wavelength of 495 nm which is in the visible range. This makes them a favourable option for NO detection in cells because visible light is less harmful to cells than UV light and they are free from interference from autofluorescence [49]. In addition, the fluorescent product is not formed in the absence of NO under physiological conditions. However, it has been demonstrated that DAF reacts with azanone [51]. Therefore, there is potential for interference by azanone which could lead to false detection of NO. Additionally,

since DAF does not react with NO directly but rather with an oxidized product of NO, the oxidation rate of NO imposes a limit on the speed of NO detection.

2.2.3 Other NO Detection Methods

Colorimetric and fluorescence techniques are the most popular for the detection of NO. However, there are a variety of other methods that exists for NO analysis. Chemiluminescence, the emission of light from a chemical reaction, can also be employed for the detection of NO. The reaction of NO with ozone (O_3) produces nitrogen dioxide (NO_2). The nitrogen dioxide produced is in an excited state, and it emits a photon when it returns to its lower energy state. Another potential method for chemiluminescence is the reaction of NO with hydrogen peroxide (H_2O_2) which produces peroxy-nitrite ($ONOO^-$), which is highly oxidative and reacts with chemiluminescence agents such as luminol[52]. A photomultiplier is used to convert the emitted photon into an electrical signal. The electrical signal is proportional to the NO concentration. Chemiluminescence is highly sensitive, can provide real-time measurements, and has been effective in measuring NO in endothelial cells. However, it cannot be used for *in vivo* measurements. Furthermore, the reaction mechanism utilizing ozone can cause problems because it is difficult to provide a repeatable and stable gas stream.

Gas chromatography is another indirect method for NO detection. Gas chromatography is based on the separation of compounds based on their physical and chemical properties in the presence of gas flow [53]. This method is used for the indirect detection of NO because of the reactivity and short half-life of NO. Therefore, the products of NO, nitrite and nitrate are measured instead. The combination of gas chromatography and mass spectrometry allows for the simultaneous detection of both products [54].

EPR or ESR (electron spin resonance) is also used for NO detection [12]. EPR is a method for the characterization of free radicals which are challenging to detect and measure because of their reactivity and short half-life. EPR transforms reactive free radicals into stable radicals through a reaction with a specific compound referred to as a ‘spin trap reagent.’ A commonly used spin trap reagent is iron (Fe) complex with dithiocarbamate derivates. EPR is an effective method for NO with many benefits, specifically its ability to provide critical information about free radicals in complex environments. However, it remains an expensive and time-consuming method.

2.3 Detection of NO with Electrochemical Tools

Electrochemical methods are interesting for the detection of NO. They can be utilized to provide both *in vivo* and *in vitro* measurements. As well, they provide direct, real-time measurements with high sensitivity and selectivity. The principle utilized for the detection of NO with electrochemistry is the measurement of the current rise by the oxidation of NO on the electrode surface. The electrochemical set-up is typically a two-electrode or three-electrode system composed of a working electrode (WE) which is used for the detection of NO, a reference electrode (RE) which provides a base potential, and counter electrode (CE) to complete the circuit. These electrodes are immersed in solution containing NO and a positive potential is applied which results in the oxidation of NO in an electrochemical redox reaction. The NO oxidized is directly proportional to the flow of current through the WE. However, the type of electrode utilized is a matter of great significance for the detection of NO with electrochemistry [12].

There were various types of electrodes that can be used for the detection of NO. Early electrodes that were used for NO detection include platinum and platinum alloys [55], [56]. The first electrodes for the electrochemical detection of NO *in vivo* appeared in 1990 a paper by Shibuki in which a platinum wire was placed in a glass micropipette filled with sodium chloride and hydrochloric acid. The end of the micropipette was sealed with a membrane that was permeable to NO [57]. In 1994 a study by Bedioui *et al.* employed gold electrodes for the NO detection in solution [58].

As the electrochemical detection of NO occurs on the surface of the electrode, the physical and chemical properties of the electrode surface is critical, particularly for the detection of analytes such as NO which are present in very low concentrations [59]. The modification of the electrode surface can increase the speed of the electrochemical reaction, increase the conductivity of the electrodes, and alter the permeability of the electrode membrane [55]. These modifications to the electrode surface can improve response time, sensitivity, and the selectivity of the sensors to NO.

The development of surface modified carbon fiber microelectrodes by Malinski and Taha in 1992 is a significant step forward for electrochemical NO detection [60]. Malinski and Taha conducted cell measurements *in situ* with a LOD of 10 nM and demonstrated a linear response up to 300 µM. In this study, the microsensors were coated with Nafion to prevent any interference because Nafion is highly permeable to NO but impermeable to anions such as nitrite and nitrate. This development

was considered an important achievement because the “size, detection limit, linear range, response time, selectivity and applicability to *in situ* measurements cannot be found in any other method for measuring NO” at the time of publication [60].

2.3.1 Hydrogels and Xerogels

Hydrogels are polymer chains that are infused with water because of their hydrophilic structure [61]. Hydrogels can be formed from natural, synthetic, or a combination of natural and synthetic polymers [62]. Hydrogels can absorb large amount of water in their interstices and maintain their structure because of crosslinking bonds. The properties of hydrogels such flexibility and adhesion and as well as biocompatibility and biodegradability make them attractive options for wound dressing [63]. NO has been demonstrated to play a role in healing wounds and injuries because of the role it plays in vascular homeostasis, cell growth and proliferation, antimicrobial action, and immune response [64], [65]. The antimicrobial effects of NO arise from its instability as a free radical which quickly forms reactive species, such as peroxy-nitrite, which can damage the cell membrane and can cause damage to DNA from which bacteria cannot defend themselves and therefore the bacteria are destroyed [66]. The short half-life and reactivity of NO mean that NO is usually provided to tissues via an ‘NO donor’ which is a molecule that releases NO. As a result, the creation of NO hydrogels to store and deliver NO to the site of injury, combining the wound healing and wound dressing functions of NO and hydrogels respectively, is an attractive idea.

There are different types of hydrogels that have demonstrated the ability to store, release and deliver NO including composite, polyvinyl alcohol (PVA) based, thermos-responsive, injectable, *in situ*, supramolecular, and hydrogel forming microneedles. As stated above, these hydrogels can be composed of natural or synthetic polymers, however synthetic polymers are less suited than natural polymers to adhesion and cell proliferation [67]. In 2023, the Meyerhoff group created an injectable hydrogel composed of the natural polymer alginate that can facilitate the controllable release of NO [68]. S-nitroso-N-acetyl-penicillamine (SNAP) functioned as an NO donor in the injectable hydrogel and the antibacterial activity of the hydrogel was correlated with the SNAP degradation over 24 hours.

Xerogels are fabricated through the evaporation of the liquid present in the pores of hydrogels at ambient temperatures [69]. Biosensors produced using xerogels have been demonstrated to be swift and highly sensitive detection of studied molecules. A fluorinated xerogel layer on carbon fiber

microelectrodes has been used *in vivo* in the brains of adult rats for the detection of NO [70]. Carbon fiber microelectrodes coated with a fluorinated xerogel layer had greater selectivity than comparable electrodes coated with a Nafion layer. This is because electrodes coated with Nafion demonstrate high sensitivity to dopamine and serotonin as Nafion is a negatively charged molecule. However, the electrodes coated with Nafion had a slightly higher sensitivity although the sensitivity results were comparable.

2.3.2 Eugenol

Eugenol (EUG) is a pale yellow, naturally occurring compound with a MW of 164.2 grams per mole. It has a chemical formula of $C_{10}H_{12}O_2$. There are various sources for eugenol including nutmeg, cinnamon, and a variety of plants [71]. EUG is also the major component of the oil extracted from cloves, a spice native to a chain of islands part of Indonesia [72]. Steam distillation is the most common method of EUG extraction, following the extraction of oil from plants. There are a variety of health benefits of eugenol consumption including anti-tumour, antioxidant, antidiabetic, and anti-inflammatory effects as well as neuroprotective and anti-microbial properties[73].

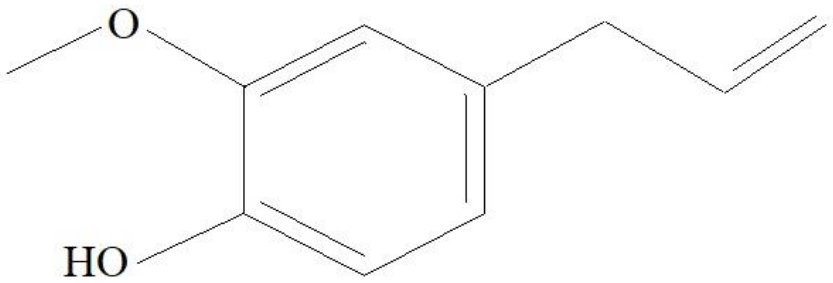

Figure 2-3: Structure of eugenol.

EUG is declared by the World Health Organization (WHO) to be generally recognized as safe (GRAS) and is biocompatible[71], [74]. Therefore, it can be used as a coating on NO sensors in biological mediums. The benefit of EUG is that it improves the selectivity of the sensors to NO [75]. This is because although other coatings to improve the selectivity of NO, such as Nafion, protect the sensors from detection interference by anionic compounds such as nitrite, they do not protect the sensors from interference from cationic molecules such as dopamine. However,

although higher concentrations of EUG result in sensors with improved selectivity to NO, they also reduce the sensitivity of the sensors to NO [74]. NO biosensors coated with EUG have demonstrated high sensitivity, selectivity, and a low LOD [74], [76].

2.4 Paper biosensors

There are several benefits of paper sensors for biomedical research and detection. Paper is an inexpensive and ubiquitous material that is portable, disposable, and easy to use [77]. Whatman filtration paper is often used for production of paper sensors because of its low cost, commercial availability, and wicking properties [65]. Paper sensors are key to acquiring information rapidly and conducting real time monitoring, particularly in low income countries [79]. Furthermore, paper is biocompatible and the porosity of paper can be manipulated for the production of paper-based microfluidic channels [80]. The Whitesides group at Harvard University investigated patterned paper that is technically simple, low-cost, and portable for bioassays [81]. The Whitesides group also studied the printing of polydimethylsiloxane (PDMS) onto paper [82]. The printing of hydrophobic materials such as PDMS onto paper creates an impermeable barrier for aqueous substances which allows for the clear definition of microfluidic channels. Paper sensors can be used for a variety of detection methods. However, most of the research on paper sensors rely on colorimetric techniques for detection [83], [84]. However, colorimetric techniques are limited in scope because of their low sensitivity, high LOD, and short linear ranges.

2.4.1 Electrochemical sensors on paper

Electrochemical sensors on paper make an attractive alternative to colorimetric sensors because they can be conducted rapidly and achieve high sensitivity and selectivity [85]. In 2009, the Henry group produced the first demonstration of electrochemical detection using paper-based microfluidics [86]. The paper electrodes were characterized using cyclic voltammetry (CV) and were tested using glucose, lactate, and uric acid. Electrochemical paper analytical devices (ePADs) have been used for the detection of metals in aerosol samples [87]. These ePADs, referred to as Janus ePADs, were used to simultaneously detect multiple metals including cadmium, lead, copper, iron, and nickel. Janus ePADs were also used to simultaneously detect two different neurotransmitters, serotonin and norepinephrine [88].

The Whitesides group combined ePADs with glucometers to rapidly analyze and quantify the glucose, cholesterol, lactate in blood and urine [89]. Paper-based microfluidic devices were also used to detect glucose, lactate, and uric acid in an artificial urine solution [90]. This was achieved with an LOD of 0.35, 1.76, and 0.52 mM for glucose, lactate, and uric acid respectively. A later study employed paper-based microfluidics devices coated with zinc oxide nanowires (ZnO NWs) to improve the sensitivity and lower the LOD to a range of 59.5-94.7 µM depending on the radii of the sensors [91].

Electrochemical sensors on paper have also been utilized in cell culture as well. Paper-based electrochemical sensors have been used for the detection of cancer cells with high sensitivity [92]. As well, a paper working electrode with platinum nanospheres grown upon it was successfully used for the real-time determination of hydrogen peroxide flux *in situ*[93].

2.5 Cell Culture

The use of the paper sensors in *in vitro* cell culture is necessary for the determination of the utility of the sensors in biological situations. Three-dimensional (3D) cell culture platforms are desirable to mimic living tissues [94]. This is particularly important for the study of cell adhesion and tumour biology [95]. 3D cell cultures on paper provide an ideal platform to model tissue and organ processes, such as angiogenesis [96]. Paper is an effective substrate for the culture of breast cancer that mimics the behaviour of the solid tumours. Furthermore, paper platforms provide an excellent control over the composition of the extracellular matrix (ECM) [97].

Endothelial cells (ECs) are ideal to study the role of NO in the angiogenic processes. Human umbilical vein-derived endothelial cells (HUVECs) were first isolated in 1973 [98]. The studies found that it was possible to culture HUVECs for up to five months and the cells could be identified by their immunological and morphological properties. EA hy926 is a continuous and permanent cell line produced by the synthesis of HUVECs with the A549 cell line [99], [100]. Weibel-Palade bodies (WPBs) are soft rod-shaped structure found in humans and rats [101]. WPBs are exclusively found in ECs and are an identifying feature of the EA hy926 cell line as they have not been discovered in any other cell line [102], [103]. A study by Bauer et al. in 1992 predicted that this cell line could prove to be a useful for modeling angiogenesis [104]. This was because of the plating of these cells onto Matrigel results in the cells forming capillary-like tubes, a process resembling angiogenesis *in vitro*.

2.5.1 Vascular Endothelial Growth Factor

The development of the vasculature is a process composed of vasculogenesis and angiogenesis which refers to the creation of the initial blood vessels and the growing of new blood vessels from the pre-existing vessels, respectively. The survival of all cells is dependent on their ability to access oxygen and nutrients. The diffusion limit of oxygen is approximately 100-200 μm[105]. Therefore, for organisms to develop beyond this size, the cells must develop new blood vessels through angiogenesis. Vascular endothelial growth factor (VEGF) is a growth factor promoting the angiogenic process [106]. VEGF is the most significant regulator of blood vessel formation or angiogenesis. It is expressed in endothelial and non-endothelial cells alike [107]. VEGF plays an important role in central nervous system (CNS), cardiovascular system, and the bone. VEGF has also been demonstrated to increase the concentration of NO[108]. VEGF was first discovered in 1983 from a study involving tumour cells. VEGF is also referred to as VEGF-A because it is the founding member of the VEGF family. Members of the VEGF family have been discovered in all vertebrate species.

However, VEGF is also highly expressed in cancerous tissues. Anti-VEGF therapy has been utilized as cancer treatment to inhibit the growth and metastasis of tumours because it can prevent the angiogenic processes which are necessary for the growth of the size of the tumour [109].

2.5.2 Angiogenesis in Cancer

The angiogenic processes play a vital role in the growth and metastasis of cancerous tumours [110]. Cancer cells develop at a rapid pace compared to non-cancerous cells which results in higher secretion levels of pro-angiogenic factors and molecules such as VEGF and NO to sustain the rapid development of cancer cells. This leads to pathological angiogenesis in which impairs the necessary stages of vascular development. The resultant tumour vasculature is highly abnormal with fragile blood vessels that produce loops, dead-ends, and have insufficient diameters [111]. This presents severe obstacles in cancer treatment as it prevents the flow of anti-cancer medication to the interior of the tumour because of leakage from the vessels [112]. Furthermore, the blood vessels that are produced are sometimes composed of a composite of ECs and cancer cells which facilitates the metastasis of the tumour to other tissues and organs [113].

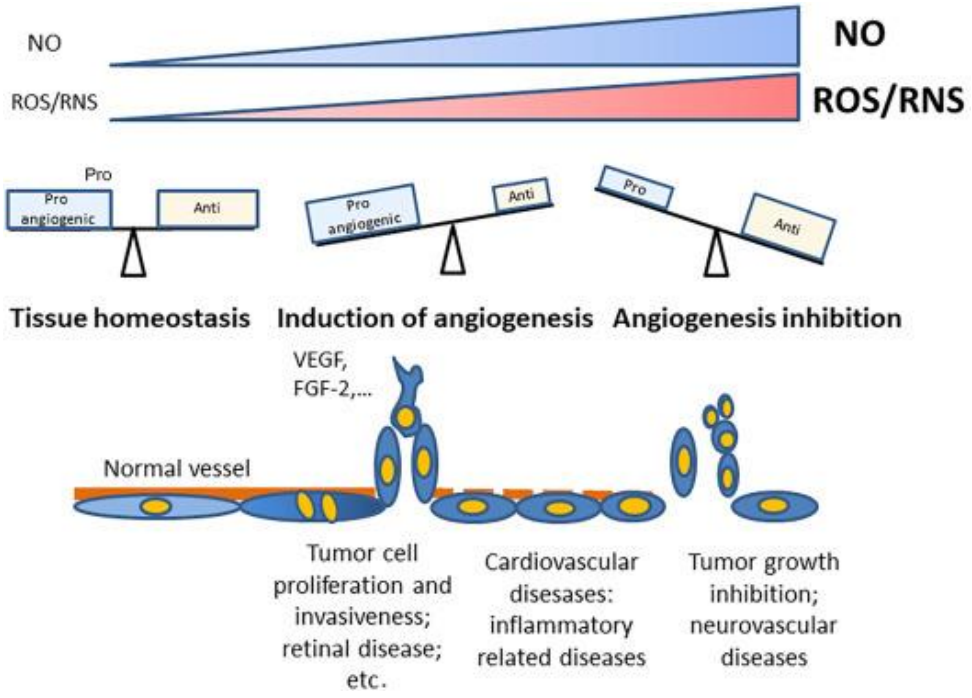

Figure 2-4: Summary of the pro- and antiangiogenic activities of NO in relation to its concentration and capacity to produce an ROS/RNS burst. Reproduced with permission[114].

CHAPTER 3 OBJECTIVES

The focus of this chapter is specifying the objectives of this study and outlining the solutions that were developed to achieve the desired objectives.

3.1 Objectives

The principal objective of this study was to fabricate paper sensors that could determine the concentration of NO in endothelial cell culture utilizing electrochemical tools.

The sub-objectives of this study were the following.

1. Fabricate paper sensors and characterize them using electrochemistry.
2. Determine the relationship between NO concentration and measured current.
3. Analyze the sensitivity, limit of detection (LOD), and selectivity of the paper sensors to NO
4. Utilize the paper sensors in biological environments, specifically endothelial cell culture, in the presence VEGF.

3.2 Solutions

This project is focused on using paper-based sensors for detecting NO using electrochemical methods. The main hypothesis of this study is that coating the carbon nanotube (CNT)-based paper sensors with eugenol will improve the sensitivity of the paper electrodes to the presence of NO and that the coating of Nafion will increase the selectivity of the sensors to NO opposed to other common biological molecules.

CHAPTER 4 METHODOLOGY

4.1 Chemicals and solutions

The chemicals that were utilized in this study were purchased from Millipore-Sigma (Canada) unless specified otherwise. The chemicals that were utilized include carbon nanotubes (CNT), Nafion, EUG, phosphate buffer solution (PBS), and DEANONO-ate, a NO-donor. The CNT ink was used as received and at the concentration provided by Millipore-Sigma and the PBS solution was prepared using the methodology specified on the package. Nafion was diluted to a concentration of 5% v/v in ethanol and the eugenol was prepared at a concentration of 0.1 mM in 0.1 M NaOH.

4.2 NO Sensor Fabrication

There were six main steps involved in the fabrication of the paper sensors. The first step was to acquire Whatman filter paper and laser cut the paper into long and narrow strips with the dimensions in the 10 mm in length and 2 mm in width using the Rayjet 50 30-Watt CO_2 laser cutter in the BASyL Lab. The parameters were optimized to cut into the paper with no discernible burn or smoke marks with a power of 3 Watts, a speed of 7.5cm/s, and a frequency of 2000Hz. The second step was to dip coat the laser cut paper strips with CNT. This was done by submerging the paper in CNT ink three times and drying the paper on a glass wafer in between each dip coating. Afterwards, the paper was placed in the oven for five minutes at 100 ºC. The third step is to insulate the working part of the electrode from the part that will be connected to the electrochemical system and the potentiostat. This task was completed by cutting long strips of parafilm and placing them across the middle section of both sides of the electrodes. The electrodes were then placed in the oven at 100 ºC until the parafilm had melted onto the paper electrodes. The fourth step was to coat the working part with Nafion utilizing the same method that was employed to coat the paper with CNT ink. The strips were dip coated with Nafion three times and left to air dry on a glass wafer in between each coating. Subsequently, the paper electrodes were placed in the oven for four minutes at 90 ºC to bake the Nafion layers. The fifth step was to cut the working part of the paper electrodes to the desired length. The desired length was approximately 2-3 mm. The electrodes were placed under a ruler and 2-3 mm from the bottom edge of the parafilm was measured and the paper electrodes were cut from that point with a scalpel knife. The final step in this process was to coat the working part of the electrode with EUG. This task was completed using electrochemical

techniques that will be discussed further in the subsequent section. The paper electrode was connected to the CHI 1040 potentiostat along with a reference electrode (RE) and a counter electrode (CE) and was placed in a small beaker containing 10 mL of 0.1M NaOH containing 0.1mM eugenol. Subsequently, cyclic voltammetry (CV) was run on the potentiostat for 25 cycles at 100 mV/s with a potential range of 0-1.25V.

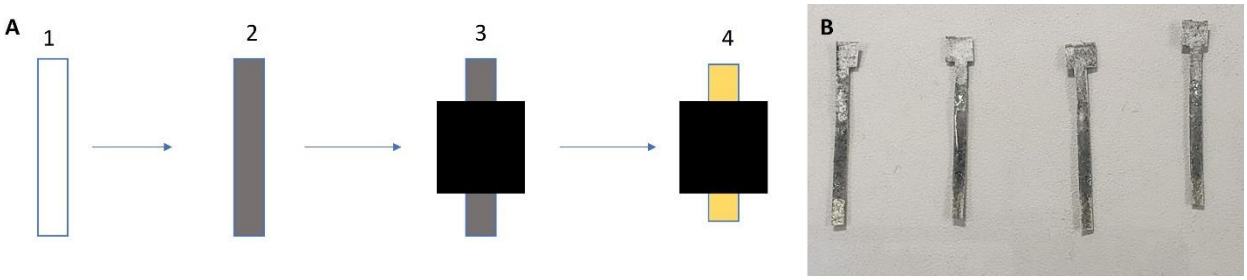

Figure 4-1: A- NO sensor fabrication process starting with 1. Whatman filter paper 2. paper coated with CNT ink 3. parafilm coated onto the middle section of the sensor 4. active part cut to 2mm and coated with nafion and eugenol and B- fabricated NO sensors.

4.3 Electrochemical Methods

The sensors were used to detect and quantify the concentration of NO in a solution using amperometry and differential pulse voltammetry (DPV) in a three-electrode system. The sensors are first placed in a blank solution containing 10 mL of PBS and the current is measured. Afterwards, the electrodes are placed in solution containing 10 mL of PBS and 100, 200, and 300 µL of DEANONO-ate which is a NO progenitor.

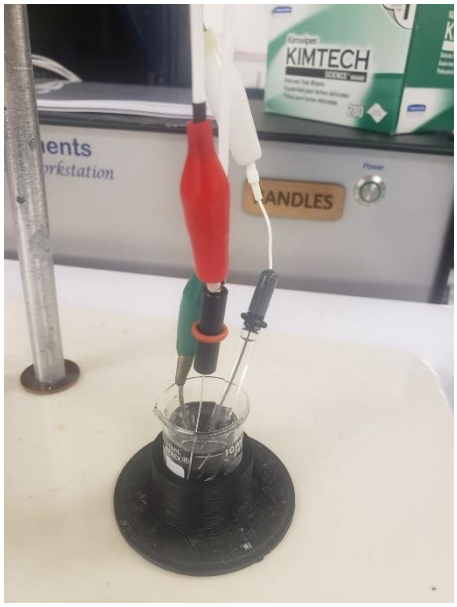

Figure 4-2: NO sensor connected to potentiostat with crocodile clips as part of a three-electrode system.

4.3.1 Three Electrode System

The electrodes were connected to a potentiostat, which is a device that controls the potential and measures the current, using crocodile clips. The electrodes were analyzed as part of a three-electrode system. The three-electrode system is composed a working electrode (WE), a reference electrode (RE), and a counter electrode (CE). The WE are the electrodes whose behaviour is being studied and, in this study, the paper sensors function as the WE. The RE is the electrode that provides a fixed base potential. The CE completes the circuit by providing a conductive path for the electrons flowing through the reaction [115]. In this system, the RE is a silver|silver chloride (Ag|AgCl in 3M NaCl) electrode and the CE is a platinum wire electrode.

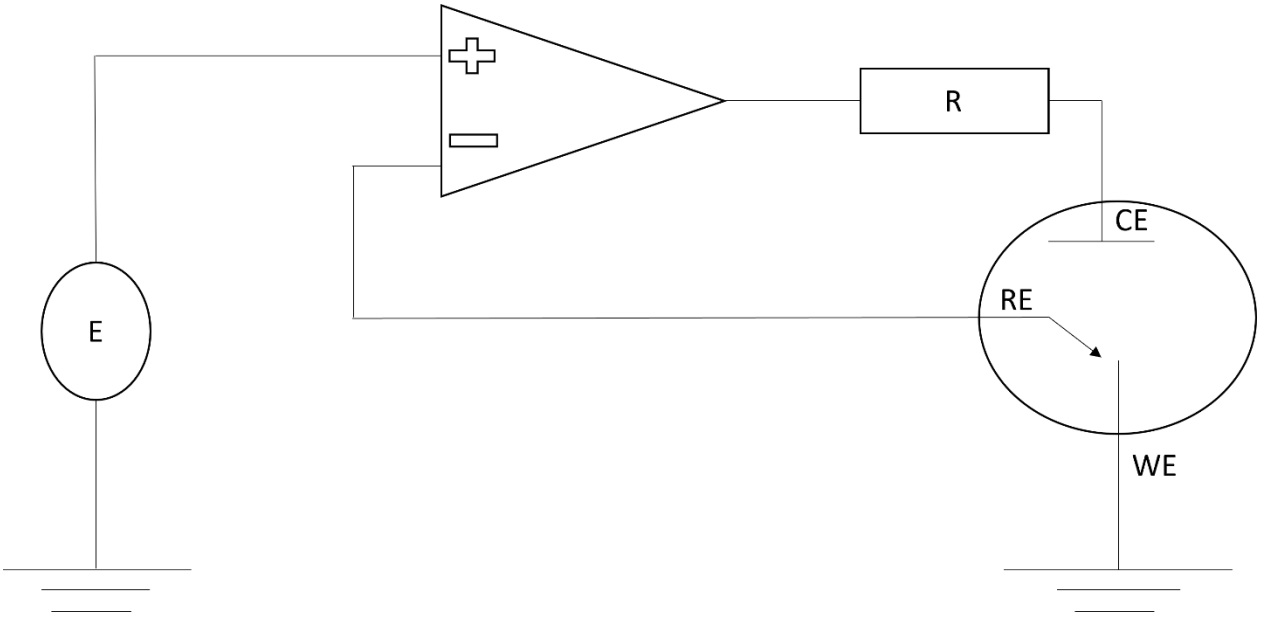

Figure 4-3: Electrical circuit schematic of potentiostat connected to a three-electrode system.

4.3.2 CV, DPV, and Amperometry

The primary methods of electrochemical analyses employed in this study to characterize the paper sensors are differential pulse voltammetry (DPV) and amperometry as well as cyclic voltammetry (CV) in the fabrication process. Voltammetry is an electrochemical process in which the potential varies, and the current is measured. CV linearly increases and decreases the potential repeatedly. This produces a cyclic voltammogram, CV. On the other hand, DPV is a slower electrochemical technique in which "small amplitude, short pulses are superimposed on a linear ramp" [116]. The parameters utilized for the DPV were 2 cycles with 0 - 1.0V for the potential with a scan rate of 100 mV/s.

Amperometry is another electrochemical technique in which the potential is fixed, and the current is measured over time. It illustrates the rise and degradation of the current within a given time frame. In this study, amperometry was utilized because NO oxidizes when exposed to oxygen and therefore the measured current could decline as the molecule was oxidized. Amperometry was used to determine whether three trials of DPV scans could be conducted, taking approximately seven minutes, without the NO being oxidized. The parameters utilized were the following. The potential was fixed to 0.9V and the time frame was 1800 s with the first five minutes (300 s) allowing the current to stabilize.

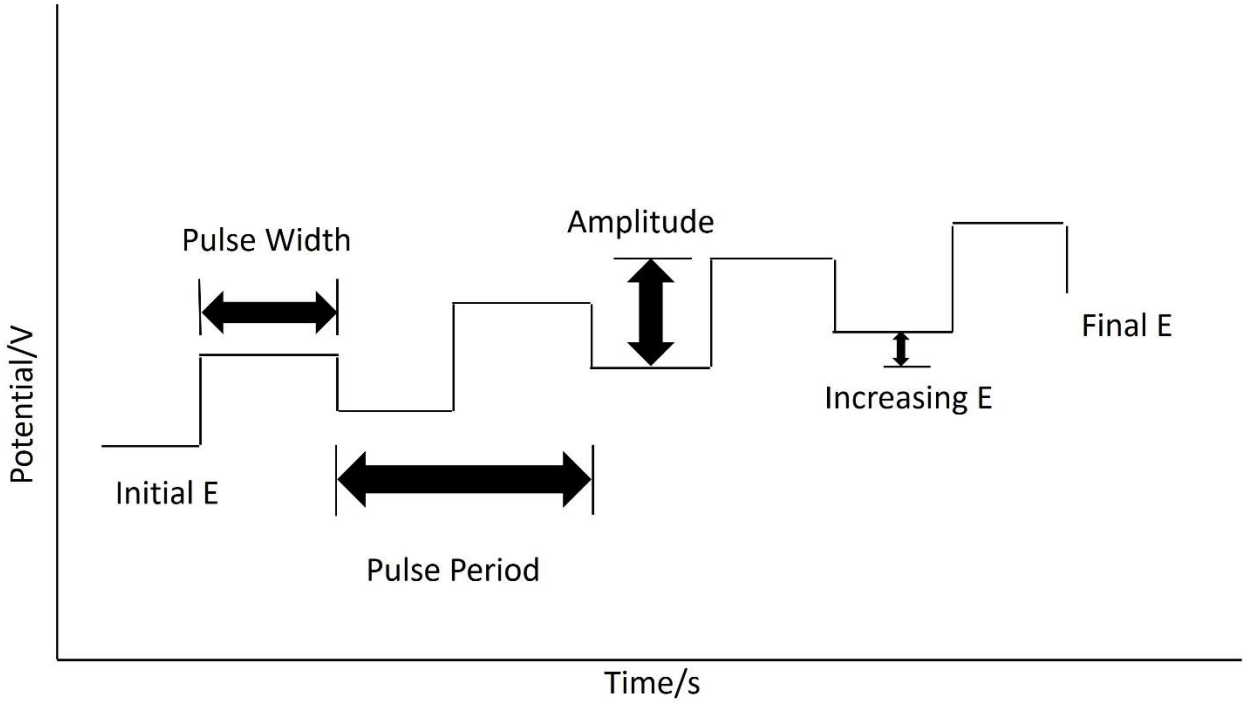

Figure 4-4: Diagram presenting the potential input waveform of DPV.

4.4 Cell Culture

After the NO sensors were characterized in chemical solutions, the sensors were utilized in endothelial cell culture to determine the efficacy of the sensors in biological environments. EA hy926 cells (purchased from ATCC) were harvested with a cell scraper. The cells in the cell culture were aspirated several times to break down cell agglomerates. The cell suspension was centrifugated at 1000 RPM for 5 mins. The pellet was resuspended in cold (4°C) extracellular matrix (ECM) gel from Engelbreth-Holm-Swarm murine sarcoma to reach a cell concentration 5 10^7 cells/ml. 2 µl of this cell suspension, containing 100,000 cells, was drop cast on the sensing part of the paper device and allowed to set on the incubator for 5 mins.

The three-electrode system was set-up in the same manner as it was done in the chemical solution The electrode with cells placed upon it was attached to the WE connection and place it in 8 mL of PBS. Afterwards, the amperometry was started with the same conditions as before for 1800s. 2 mL of VEGF was added to the solution after ~five minutes (300s, which was used to allow the current to stabilize) to reach a final concentration of VEGF of 100 $ng.ml^{-1}$. The amperometry was run for the remaining 1500s.

4.5 SEM and XPS

The fabricated paper sensors were analyzed under the scanning electron microscope (SEM) The SEM utilized was the Quattro ESEM in the CM^2 service in Polytechnique Montreal. The paper sensors were examined at each stage of sensor fabrication. The images were taken of blank Whatman filter paper, paper coated with CNT ink, paper coated with CNT and Nafion, and lastly finished electrodes with CNT ink, Nafion, and electropolymerized eugenol.

The sensors were also analyzed using X-ray photoelectron spectroscopy (XPS). XPS is a high vacuum surface analytical tool is based on the photoelectric effect in which electrons are emitted from surfaces irradiated by light. It is a method that is used for surface chemical characterization that provides information about the surface chemistry, elemental composition, and bonding structure of a material [117]. The XPS that was utilized was the VG ESCALAB 250Xi in Polytechnique Montreal and were analyzed at the same four stages as the SEM. The paper sensors were attached to insulating substrates and the spectra were analyzed using Avantage v6.5 with all high-resolution peaks fitted using symmetrical Lorentzian/Gaussian peak functions[118].

4.6 Data Analysis

The data acquired using the CHI 1040 potentiostat (CHInstruments, Texas, USA) was analyzed using MATLAB R2022a and the data values are reported as the mean ± the standard deviation, or as the median value. The sensitivity of the electrodes is defined as the slope of the linear fit of the current and NO concentration calibration curve. The limit of detection (LOD) was defined as the detected current in the blank solution plus three times the standard error and then divided by the sensitivity. The sensitivity and LOD values for the electrodes studied in this research is presented in Appendix A. The concentration of NO present in a sample following an injection of DEANONO-ate was calculated using an ordinary differential equation provided in study conducted by Griveau *et al*. in 2007 at the University of Paris [119]. The calculations and the values for the maximum NO concentration from the injection of the concentration of DEANONO-ate that was conducted in this study is available in Appendix B.

CHAPTER 5 ARTICLE 1: PAPER SENSORS FOR THE MEASUREMENT OF NITRIC OXIDE RELEASE FROM ENDOTHELIAL CELLS

5.1 Presentation of Article 1

This chapter will present the article titled “Paper sensors for the measurement of nitric oxide release from endothelial cells.” This article was submitted on May 10th, 2024, to Sensors and Diagnostics, a scientific journal published by the Royal Society of Chemistry. This journal is focused upon sensors, sensing devices, and systems.

5.2 Paper Sensors for the Measurement of Nitric Oxide Release from Endothelial Cells

Syed Hassan Ali[1] and Raphaël Trouillon[1,2,3,*]

[1]*Department of Electrical Engineering, Polytechnique Montréal, Montréal, QC, Canada*

[2]*TransMedTech Institute, Montréal, QC, Canada*

[3]*SNC research Group, Montréal, QC, Canada*

**: corresponding author raphael.trouillon@polymtl.ca*

Abstract: Nitric oxide (NO) is a ubiquitous and important biological mediator. However, its detection and chemical analysis are challenging due to its short lifetime in biological conditions. Paper-based nitric oxide (NO) sensors combining the ease of fabrication and affordability of paper to the quantitative capabilities of electrochemical methods are presented for the detection and quantification of NO in cultured cells. Nafion-coated and eugenol-functionalized paper were built and characterized using a NO-donor. The electrochemical interferences from nitrite, a common interferent for NO sensing, were successfully screened out. Finally, preliminary data were obtained from 100,000 endothelial cells cultured directly, in an extracellular matrix, on the paper device. In response to vascular endothelial growth factor exposure, NO secretion was detected and quantified.

Keywords: nitric oxide, paper devices, electrochemical sensors, vascular endothelial growth factor, endothelial cells

5.3 Introduction

Nitric oxide (NO) is a ubiquitous biological mediator, a compound released by endothelial, neuronal, immune, and other cells to allow them to communicate with one another.[1–5] It is a key component of efficient immune response,[3,6] and a critical agent in the regulation of blood pressure and angiogenesis, the growth of new blood vessels.[7,8,8] However, extremely high rates of a NO synthesis is associated with adverse health conditions including cancer.[2,9] Tumors are typically highly angiogenic structures, containing high levels of growth factors.[10,11] One of these families of molecules, vascular endothelial growth factors (VEGF), activates endothelial cells into an angiogenic state and stimulates the secretion of NO.[7] VEGF is thus a clinical target, and anti-

VEGF therapies are being used clinically.[12] Therefore, the quantification of NO release may be useful in the diagnosis of cancer as well as determining the efficacy of different cancer treatments.

Unfortunately, the quantification of NO is challenging, especially in a biological context, owing to its short lifetime in physiological conditions as it is quickly oxidized to nitrites.[13] This rapid scavenging has complicated the accurate measurement of NO levels and thus impeded its precise study. Amongst the most common methods for NO detection and quantitation, the Griess test is a colorimetric assay.[14] This method oxidizes NO to nitrites and measure the nitrite levels. This two-step strategy limits the selectivity of the assay, as endogenous nitrites are included in the readout, and are not compatible with fast, *in situ* analyses. Similarly, diaminofluoresceins are fluorescent compounds for NO detection.[15] They are suitable for fast microscopic assays, but are also prone to limited selectivity.[16]

Electrochemical methods are attractive solutions for biosensors owing to their adaptability to a wide range of samples and measurement scenarios, sensitivity, low cost and rapid response time.[17–19] As NO is electroactive, it can be readily oxidized on a wide range of substrates and several NO electrochemical sensors have been proposed. Malinski's work highlighted the usefulness of porphyrinic compounds,[20,21] and eugenol-based electrodes have been proposed for the measurement of NO released by neurons.[22] There have been significant improvements in the past decade in the detection of NO with significant improvements in the selectivity, sensitivity, sensocompatibility, and cytocompatibility. [17] Limits of detection (LoD) of few nM have been reported with modified carbon microelectrodes.[22] However, most of these techniques are specialist solutions that limit the dissemination of the technology.

Paper-based biochips have attracted significant interest over the last decade.[23–27] Paper is here used as a substrate for handling liquid passively, taking advantage of the capillary action of porous paper, but also for adding sensors, electronic or mechanical components. The wicking action of paper is particularly useful as it allows for pumpless microfluidics. Paper is easy to handle, cut and functionalize and is highly amenable to a wide range of bioassays.[23,28,29] The integration of electrochemical sensors has been demonstrated on several types of paper substrate.[30–34] These electrodes are usually made from conductive inks or polymers (*e.g.* PEDOT-PSS solutions, carbon nanotubes (CNT) or graphite suspension, *etc*.) deposited or printed directly on the paper.[35,36]

However, there are several limitations to paper-based electroanalytical devices.[37] The opacity of paper hinders the use of microscopy. Fluorescence microscopy or openings in the paper can help circumvent this issue.[38] The size of the features deposited on the paper is limited by the characteristics of the paper surface, *i.e.* the size of the pores (in the 10 to 100 μm range, depending on the paper). This sets a limit to miniaturization of features on paper substrates, even though specialized papers for printed electronics are available. The random nature of paper, especially the filter paper used here, can also impact the reproducibility of the devices. Finally, as the conductive structures are often printed and/ or deposited as a thin layer on the cellulose substrate, these thin-film electrodes can typically show a lower conductivity than traditional ones. It has been found that maintaining small electrode dimensions can help limit the drop in potential in the device.[32] Electrode designs with low aspect ratios are better that ones with large aspect ratios, probably as it improves conductivity, but keeping overall all the dimensions as small as reasonably possible (typically 1 to 2 mm) led to the best electrode response, possibly by lowering the electrode capacitance.[32] The smallest electrode dimension is set by the typical pore size (the device must be significantly larger than this distance to overcome the paper surface randomness) and the specifications of the laser beam. It also reduces the amount of reactant needed to functionalize the device. Taking these limitations into account, paper can nevertheless be used to build efficient sensors benefiting from ease of use and fabrication, as well as passive fluid handling *via* capillary action.

Importantly, cell culture on paper substrates has been well described.[39] Here, cells are suspended in gel of extracellular matrix (ECM) and the solution is then spotted on paper. As the gel solidifies, an ECM matrix containing cells is maintained in the pores of the paper (typically a filter or chromatography paper), which here acts as a scaffold providing mechanical strength to the fragile gel. The resulting construct is a 3D cell structure that can be used for studying the cellular response to hypoxia, or testing drugs.[40,41] It has been reported which electrochemical sensors that these samples can be easily integrated into microfluidic chips and describe well the neurochemical response of the cells to stimulation,[42] or the ability of muscle cells to capture glucose when exposed to insulin.[43] The possibility to combine electrodes on paper to cell culture in the same paper device has recently been reported, and used to test different neurosecretion altering drugs.[38]

In this study, paper-based sensors are fabricated and tested in varying concentrations of NO. The devices were also characterized with scanning electron microscopy (SEM) and X-ray photoelectron

spectroscopy (XPS). The final devices were calibrated and tested against common interferences. Finally, preliminary results showing the possibility of seeding endothelial cells onto the paper devices and observing their secretion of nitric oxide in response to VEGF exposure are reported.

5.4 Methodology

5.4.1 Chemicals and solutions

Unless stated otherwise, all the reactants were purchased from Millipore-Sigma (Canada). Deionized water was used throughout the experiments (resistivity 18 MΩ cm). The CNT ink is a commercial aqueous suspension of single walled CNT (0.2 mg/ml, ref. 791490). The solution is supplemented with sodium dodecyl sulfate (SDS) to prevent aggregation of the nanotubes.

5.4.2 Electrochemical setup

All the electrochemical measurements were run with a CHI 1040C potentiostat (CHinstruments, TX, USA). A 3-electrode setup was used, with a Pt counter electrode and an Ag|AgCl (3M NaCl) reference electrode. All the electrode potentials are reported *vs.* Ag|AgCl (3M NaCl). In some experiments, 3-mm glassy carbon (GC) electrodes were used after polishing them with 0.03µm alumina slurry.

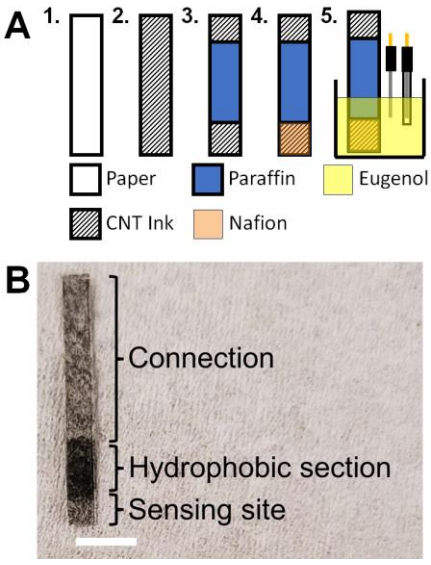

Figure 5: Fabrication of the NO sensors. A- Schematics showing the preparation protocol: 1. Cutting paper pieces, 2. coating in CNT ink, 3. blocking part of the paper with paraffin, 4.

depositing Nafion and 5. electropolymerizing eugenol. B- Photograph of the final device, showing the different parts of the paper electrode (the scale bar shows 1 cm)

5.4.3 Paper electrode fabrication

Whatman filter paper was laser cut using a Trotec laser cutter to create paper electrodes (Figure 5A). The paper electrodes were coated with the CNT ink.[31] The electrodes were dip coated in CNT three times and air dried after each coat by placing the paper electrodes on a glass slide. The electrodes were then placed in the oven for five minutes at 90°C. 3-4 mm-wide strips of parafilm were melted onto the paper electrodes by placing them on the paper, and then placing the paper electrodes into the oven at 100°C until the parafilm has melted. This section of melted paraffin is used to limit the active site of the electrode,[44,45] and prevent the capillary wicking of the test solution along the length of the paper electrode, as it could interfere with the connection to the potentiostat (see Figure 5A). The active part of the electrode was cut to a length of 2 mm to complete the paper device (Figure 5B).

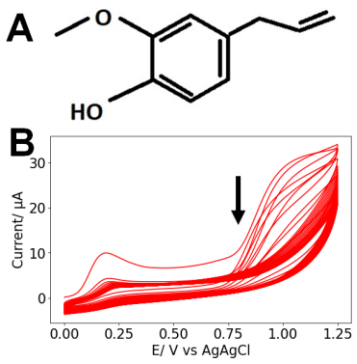

Figure 6: A- Chemical structure of eugenol. B- Typical CVs recorded during the electrodeposition of 0.1 mM eugenol in 0.1M NaOH (25 cycles, SR=100 mV s^{-1}). The arrow indicates the order of the scans.

5.4.4 NO Sensor functionalization

The NO sensing functionalization was adapted from a published report.[22] The paper electrodes were coated with Nafion by dipping them three times in 5% v/v Nafion in ethanol solution and air drying after each coating. Afterwards, the electrodes were placed in the oven at 90°C for four minutes. The electrodes were placed in 0.1mM eugenol (see structure in Figure 6A) in 0.1M NaOH.

Cyclic voltammograms (CV) were run for 25 cycles at a scan rate *SR*=100 mV s^{-1} between 0 V and 1.25 V (Figure 6B).

5.4.5 SEM and XPS analyses

SEM images of the different samples were acquired with a Quattro ESEM microscope. The sensors were also analyzed using x-ray photoelectron spectroscopy (XPS). A VG ESCALAB 250Xi was used to acquire XPS spectra. The paper sensors were attached to insulating substrates and the spectra were analyzed using Avantage v6.5 with all high-resolution peaks fitted using symmetrical Lorentzian/Gaussian peak functions.

For both SEM and XPS, the paper sensors were examined at each stage of sensor fabrication: blank Whatman filter paper, paper coated with CNT ink, paper coated with CNT and Nafion, and lastly finished electrodes with CNT ink, Nafion, and electropolymerized eugenol.

5.4.6 NO electrochemistry

All the NO electrochemistry was performed in aerated PBS at room temperature. For the initial characterization of the system three repeats of differential pulse voltammetry (DPV) were run between 0 V and 1 V in PBS. Diethylamine NONOate (DEA-NONOate), a NO donor, was used as a NO source. Once exposed to a neutral pH, DEA-NONOate spontaneously releases NO molecules in a time- dependent manner.[46] A 10 mM-stock solution of DEA-NONOate was prepared in 0.01 M NaOH.[46] Different aliquots of this stock were pipetted into 10 mL of PBS to reach 100 µM, 200 µM or 300 µM final concentrations of DEA-NONOate. Three DPV were then run again with the same conditions to calibrate the sensor.The rate of the production and degradation of NO from DEA-NONOate was also analyzed with amperometry at 0.9V with a runtime of 1800 s. The first 300 s were used to allow the system to stabilize in PBS. Afterwards the DEA-NONOate was injected into the PBS ([DEA-NONOate]= 100 µM, 200 µM or, 300µM) and the current was measured for 1500 s. The baseline due to sensor stabilization was subtracted to isolate the contribution of the Faradic NO current.

5.4.7 Simulation of NO release

In addition to the experimental measurements, the kinetics of NO release from DEA-NONOate were computed using MATLAB. The concentration profile of NO release was calculated using the

differential equation provided by Griveau *et al* for the kinetics of NO release from DEA-NONOate: [46]

$$\frac{d[NO]}{dt} + k_2'[NO]^2 = k'e^{-k_1 t}$$

where $k_2' = 4k_2[O_2]$, $k_2 = 2 \times 10^6 M^{-2}s^{-1}$, $[O_2] = 1.3 \times 10^{-3} atm^{-1}$, $k' = v_{NO}k_1[NONOate]_0$, $v_{NO} = 1.5$, and $k_1 = 28.5 \times 10^{-4}s^{-1}$.

5.4.8 Cell culture and measurements

The immortalized endothelial cell line EA.hy926 (from ATCC) was used as a vascular model. The cells were grown sub-confluently in DMEM supplemented with 10% fetal calf serum in a humid incubator, 5% CO_2, 37°C. The medium was changed every other day, and the cells were passaged weekly, up to 10 passages.

To measure NO release in endothelial cells, 100,000 cells in 2 µl ECM gel from Engelbreth-Holm-Swarm murine sarcoma were deposited on the sensing part of a paper NO sensor. The ECM was allowed to set for 5 mins in the incubator, and the sensing extremity of the chip was then placed in warm medium for ~1 hr, in the humid incubator.

To run the experiment, the device was placed in warm (37°C) PBS, an amperometric measurement was initiated at 0.9 V. After baseline stabilization (~100 s), VEGF was added to a final concentration of 20 ng ml^{-1}.

5.4.9 Fluorescence microscopy

After allowing the ECM gel to set, the cells on the paper electrodes were fixed in 3.7% methanol-free formaldehyde solution in PBS for 15 minutes at room temperature. Next, the cell membranes were permeabilized in 0.1% Triton™ X-100 in PBS for 15 minutes, and the PBE were next incubated during 40 min with Alexa Fluor™ 488 Phalloidin (ThermoFisher). Between each step, the samples were washed twice in prewarmed (37°C) PBS.

After staining, the cells were imaged with a Nikon Eclipse TiE inverted C2 epifluorescence microscope fitted with a 20X objective, and z-stacks were acquired. ImageJ was used to process the micrographs. To better observe the paper geometry, differential interference contrast (DIC) was used to image the general topology of the sample. The DIC image was inverted and is here reported

in blue to highlight the position of the paper fiber. The contrast of the images was modified to better show the position of the cells in the paper fibers.

5.4.10 Data Analysis

The sensitivity of the electrodes is defined as the coefficient of the NO concentration in the linear fit. The LoD of the sensor was calculated as the concentration associated to thrice the standard deviation of the blank current. In the case of the NO amperometric measurement, the data was smoothed with a Savitsky-Golay filter, and the baseline was subtracted after a linear fit. Unless specified otherwise, the data is presented as mean ± SD for *N* measurements. Where applicable, datasets were compared using a two-tailed Student's t-test.

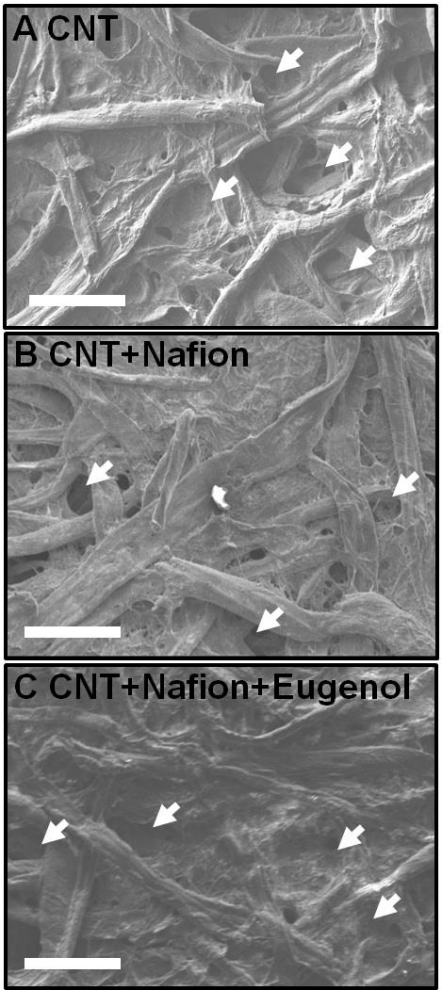

Figure 7: Typical SEM images for different paper preparations A- paper/ CNT, B- paper/ CNT/ Nafion and C- paper/ CNT/ Nafion/ eugenol. (the scale bars are 100 μm). The arrows highlight the presence of large pores on all the micrographs.

5.5 Results & Discussion

5.5.1 SEM imaging

Typical SEM images of the different samples are shown in Figure 7: the paper/ CNT, paper/ CNT/ Nafion and paper/ CNT/ Nafion/ eugenol assemblies. In all cases, the larger paper (cellulose) fibers can be observed, with a coating of CNT covering the cellulose and, in some cases, filling the pores. The addition of Nafion or eugenol does not lead to significant changes in surface texture or structure. Importantly, in all the samples observed, the paper devices retained a high level of porosity (as indicated by the arrows in Figure 7). This is critical for cell culture as the cells are maintained in the bulk of the paper, between the cellulose fibers.

5.5.2 XPS analysis

The XPS data for different electrode preparations is shown in Figure 8. As the CNT ink is deposited on the pristine paper, Na 1s (1071.2 eV) and S 2p (169.0 eV) peaks are observed. This is attributed to the presence of SDS in the CNT ink. The electrode is then encapsulated in Nafion, a fluorosulfonic acid, as revealed by the presence of an F 1s peak (688.8 eV). Finally, after eugenol deposition, the relative height of the F 1s peak vs the O 1s peak is greatly reduced. The Si 2p (102.4 eV) and Si 2s (174.5 eV) peaks are likely contamination due to silicon leaking from the glassware containing the alkaline eugenol solution (in 0.1 M NaOH). This analysis confirms the successive deposition of the different layers of the NO paper sensor.

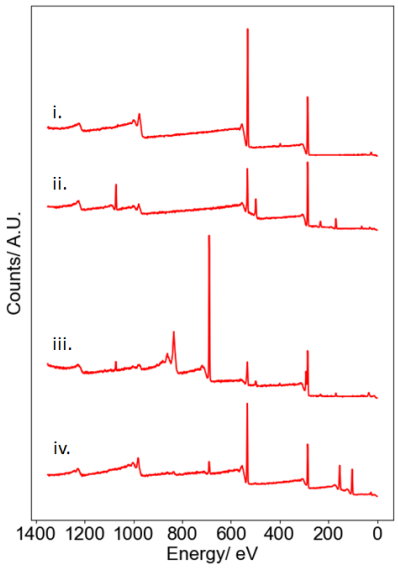

Figure 8: XPS traces obtained for i. pristine paper, ii. paper with CNT, iii. paper/ CNT/ Nafion and iv. paper/ CNT/ Nafion/ eugenol.

5.5.3 Kinetics of NO release from DEA-NONOate

DEA-NONOate was used as en easily accessible, source of NO. Each molecule theoretically releases 2 molecules of NO once at physiological pH, but previous studies highlighted that this release is incomplete and not instantaneous, as highlighted in Figure 9A-C. To better understand these dynamics, the maximum [NO] released from different starting concentrations of DEANONO-ate was computed (Figure 9D).[46] As previously reported, the relationship between [DEANONO-ate] and the maximum [NO] non-linear. Table 1 presents the maximum concentration $[NO]_{max}$ and the instant when that maximum is reached t_{max} computed from these simulations for the 3 concentrations used in the experiments.

Table 1: Parameters obtained from the ODE computation for the release of NO from DEA-NONOate as described in [46].

[DEA-NONOate]/ µM	100	200	300
$[NO]_{max}$**/ µM**	13.6	18.7	24.5
t_{max}**/ s**	89.8	57.5	41.6

To confirm these results experimentally, the amperometric response of the paper sensors in the presence of varying [DEANONO-ate] was obtained. The amperometric current (Figure 9E), recorded at 0.9 V, increases rapidly thus confirming the sensitivity of the paper devices towards NO. Figure 9E presents the amperometric data recorded for 100 μM of DEANONO-ate and the corresponding simulation. In both cases, a sharp rise in current or [NO] is observed, followed by a slow decrease. However, these kinetics are much faster in computation in comparison to the experimental data. This could be evidence of complex, hindered mass transport of the DEANONO-ate in the pores of the paper and the Nafion layer leading to diffusive dispersion of the peak.

To investigate this possibility, the ODE solution for 100 uM DEA-NONOate was convoluted with a Gaussian function to simulate a hindered diffusion pathway. The width of the Gaussian was adjusted so that the maxima of the diffusively hindered ODE and the experimental amperometric trace match. The fit was optimal for a 340-s Gaussian width, which likely arises from tortuous diffusion in the paper matrix. This diffusion time t_{diff} which can be associated to a diffusion distance $x_{diff} = \sqrt{2Dt_{diff}}$ where D is the diffusion coefficient, for unidimensional diffusion. DEA-NONOate, whose structure is $C_4H_{10}N_3NaO_2$, has a molecular weight of 209.6 Da. Assuming a diffusion coefficient of 10^{-10} m^2s^{-1} for DEA-NONOate, t_{diff} = 340 s is associated to x_{diff} = 261 μm. As the Whatman 114 paper is 190 μm-thick, this analysis hints that the peak broadening observed in Figure 9E can be associated with slower diffusion of the NO-donor in the bulk of the porous paper coated with the Nafion film. Slower diffusion due to higher tortuosity in partially blocked media has been well described.[47,48]

To investigate the impact of the porous structure of paper on the detection kinetics, a GC electrode was used to prepare a NO sensor, using the same protocol. This results in a flat sensing surface, with properties similar to the paper device. In this case, the current increase following DEA-NONOate addition is faster, as it reaches its maximum earlier, and decays more rapidly, than for the paper device (Figure 9F). However, the observed current for GC is still slower than the profile predicted by the ODE. This indicates that i- the structure of the paper and ii- the Nafion layer both decrease NO detection kinetics, probably because of diffusional hindrances.

Despite these slower kinetics, DEA-NONOate provides an easy source of NO, as demonstrated by amperometry. Importantly, it was found that [NO], thanks to the peak broadening, was relatively

stable over the course of the voltametric tests described below (>600 s) and is therefore suitable for the calibration of the paper NO sensors.

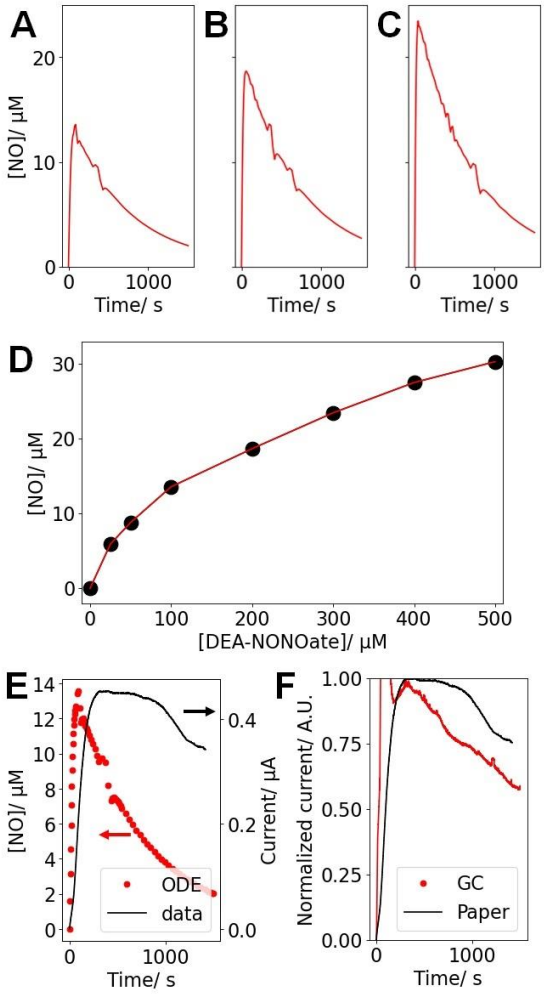

Figure 9: Results of the ODE describing the [NO] released by DEA-NONOate for starting concentrations of A- 100 µM, B- 200 µM and C- 300 µM of DEA-NONOate. D- Peak NO concentration $[NO]_{max}$ for different [DEANONO-ate], as computed from the ODE described in [46]. E- Comparison of the ODE for [DEA-NONOate]= 100 µM and the typical corresponding amperometric trace (at 0.9 V) recorded with a paper sensor after the addition of 100 µM DEA-NONOate to PBS over ~1500 s. F- Comparison of the amperometric data (at 0.9 V) recorded with a paper sensor after the addition of 100 µM DEA-NONOate to PBS over ~1500 s and obtained with a GC and a paper electrode, both prepared as NO sensors following the reported protocol. For the GC data, an injection artifact is observed in the first ~100 s, and was not considered in the analysis.

5.5.4 Voltametric characterization

The sensors were also characterized with DPV to better understand their detection mechanisms. As a reference, the NO-sensing layers (Nafion, then eugenol) were deposited on GC electrodes (Figure 10A). For this preparation, and as reported by others, a clear peak appears at ~0.7 V for NO, and its magnitude increases with [NO]. This confirms the NO sensing capabilities of eugenol on carbon electrodes.

If GC is replaced by a paper device coated with CNT, a very slight peak can still be observed in the same region but is very hard to resolve and cannot be used for analysis (Figure 10B). This is expected to be due to the higher electrode resistance of the paper devices, in comparison to the traditional GC, leading to peak broadening, as observed with other paper electrodes[31,32,38] or very thin layer electrodes. However, a consequence of this peak broadening is that the overall DPV trace appears to be shifted towards higher currents as [DEANONO-ate], and therefore [NO], increases. The current recorded at the higher potential limit of the DPV, here at 1 V, was found to be a reliable marker of [NO]. Calibration curves were therefore constructed for each paper device from the DPV current recorded at 1 V. A similar potential (0.9 V) was used for the amperometric measurement to overcome the electrode resistivity.[32] An example of such calibration curve is presented in Figure 10C.

The same calibration procedure was repeated for n=11 electrodes and the calibration curves were obtained. Overall, these 11 calibration curves displayed a linear behavior, making it possible to interpolate the electrode response between 0 and 13.8 μM. These datasets were pooled to extract the general analytical behavior of the paper NO sensors. This approach was chosen as paper devices are fragile. It is thus necessary to limit the number of calibration measurements for a single device. This also allows for overcoming the sensor-to-sensor variability due to the random nature of paper. Overall, a general calibration curve is built for this sensor fabrication protocol, allowing for then using new sensors without calibration before the cell measurements. The sensitivity and the LoD associated to each paper electrode were computed. The median, 1st and 3rd quartiles for this non-parametric set of results are presented in Table 2.

Table 2: Experimental results for the sensitivity and LoD of paper electrodes. The data presented here are for n= 11 electrodes calibrated independently.

	Median	Quartile 1	Quartile3
Sensitivity/ µA.M^{-1}.mm^{-2}	488.3	366.8	776.9
LoD/ µM	1.7	1.4	2.3

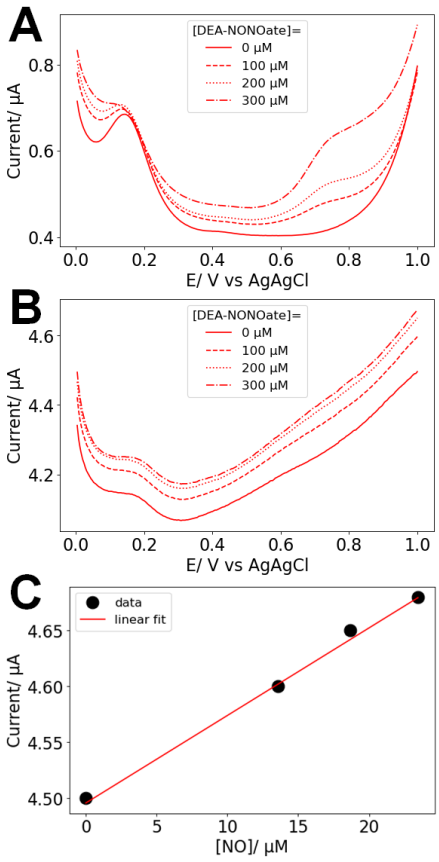

Figure 10: Typical DPV recorded in PBS, control of supplemented with 100, 200, and 300 µM of DEA-NONOate for A- glassy carbon and B- a typical paper NO sensor. C- DPV calibration curve for the data recorded from the typical NO sensor presented in B-.

5.5.5 Interferences

The signal recorded from DPV in 13.8 uM solutions of potential interferents were collected and compared to those obtained for 100 µM DEANONO-ate, corresponding to 13.8 µM NO, as presented in Table 3.

A critical requirement for NO sensing is high selectivity, especially in presence of other nitrogen-based compounds. Nitrite NO_2^- is an electroactive product of NO oxidation and should be

considered as the primary potential interferent. Here, a 2.7% level of interference is expected, hinting good screening from the Nafion layer. Nafion is a negatively charged polymer, and efficiently blocks anions such as NO_2^-. Similarly, nitrate, hydrogen peroxide or ascorbic acid, an important biological antioxidant, did not lead to significant interferences.

However, neurotransmitters were found to produce higher interferences. The molecules are typically found in the brain where they mediate neuronal communication and can be readily oxidized on carbon electrodes. Dopamine and serotonin, two important neurotransmitters, were associated with 60.0% and 13.3% levels of interference, respectively. However, neurotransmitters are more likely to be found in neuronal samples, and in specific parts of the brain associated with their release. This tissular and spatial selectivity ensures that they are unlikely to interfere with NO measurements in vascular models. Overall, the interference results agree with previous reports.[22]

Table 3: Relative response recorded from DPV run with the paper NO sensors in presence of potential interferent molecules vs. the signal obtained for 13.8 μM of NO.

Compound	**% response**
Nitrite	2.7
Nitrate	2.4
Hydrogen peroxide	14.0
Ascorbic acid	6.7
Dopamine	60.0
Serotonin	13.3

5.5.6 VEGF-stimulated NO release

For the cell measurement assay, 100,000 EA.hy926 cells were cultured directly in the pores of the paper in ECM. These immortalized hybrid endothelial cells were reported to secrete NO in response to VEGF.[49] The volume of the (cells+ECM gel) is 2 μl. SEM images were obtained for

the paper electrodes combined with ECM and cells (Figure 11A, B). The micrographs reveal that the fibrous structure of paper can still be observed, but the well-defined pores seen in Figure 7 are now filled with gel. The ECM gel here appears as a smooth coating featuring several cracks and fractures (indicated by arrows in Figure 11A,B). These are likely due to the gel drying and shrinking in the high vacuum environment of the SEM. The cells themselves are not visible in these images, as they are embedded in the gel. Overall, the SEM investigation shows a high integration of the gel in the paper, as the ECM adheres well to the cellulose fibers and fills the pores of the device. The porous nature of the paper is thus critical to produce a 3D cellular construct, maintained in the cellulose fiber lattice of the paper. This confirms that the cell-on-paper approach allows for full integration of the biological component in the paper matrix. The absence of gaps or spaces between the gel and the paper hints at fast diffusion of molecules secreted from the cells to the sensor.

To directly observe the cells maintained in the gel, epifluorescence imaging was performed (Figure 11C). The phalloidin stain marks the actin cytoskeleton, thus revealing the general shape of the cell. This image confirms that the endothelial cells are in the bulk of the paper (not only on the surface), between the fibers, in small clusters or as individual cells This furthers stresses the importance of the porous structure allowing for cells to be cultured in a 3D matrix, surrounded by electrochemical sensors deposited on the cellulose fibers.

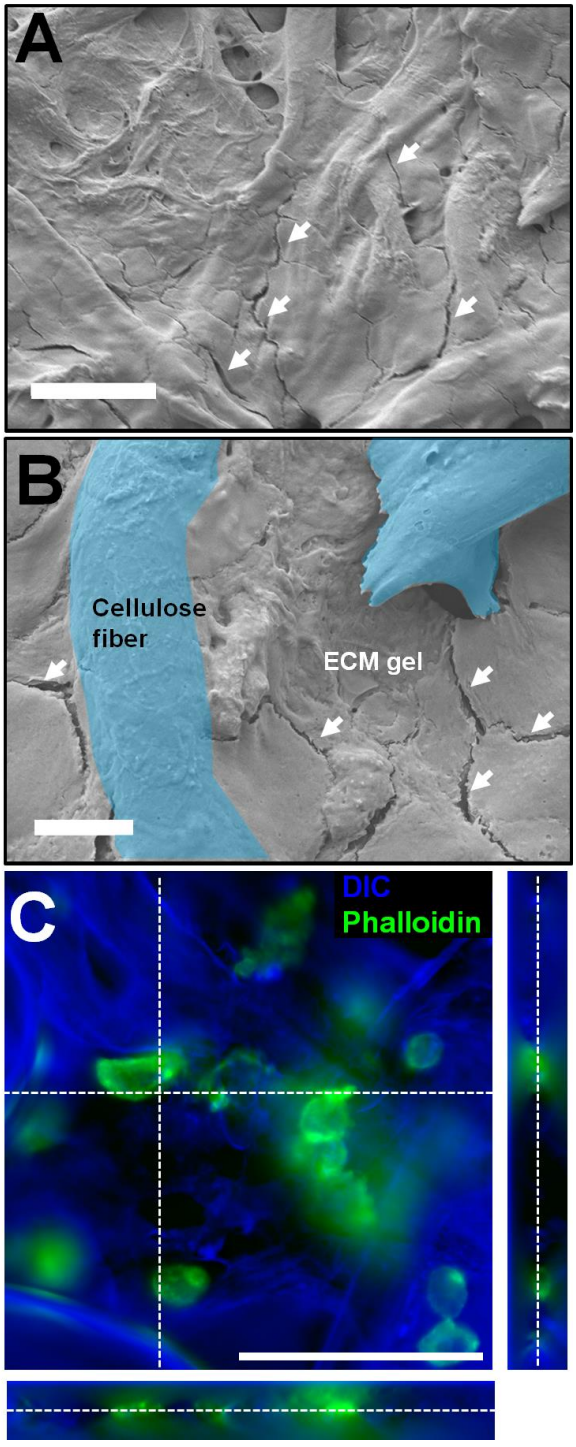

Figure 11: Microscopy of the paper devices prepared with EA.hy926 in ECM gel. A, B- SEM images of the cell and gel-loaded paper chip (the scale bars show A- 50 μm and B- 10 μm). On both panels, the white arrows highlight the presence of fissures, that are an indication of the presence of the ECM gel coating the paper fibers. In B-, two cellulose fibers (paper) are highlighted in blue (false colors), underlining how the gel fills the pores and coats the paper fibers. C- Fluorescence micrograph of EA.hy926 maintained on paper. The actin cytoskeleton

appears in green (phalloidin staining) and the topology, mostly the paper fibers, appear in blue (inverted DIC). The scale bar shows 100 µm, the stack is 50 µm-thick

Figure 12A and B present averaged amperometric measurement (at 0.9 V, n=3 for each case) for paper devices without and with 100,000 EA.hy926 in ECM gel, following stimulation with 20 ng.ml^{-1} VEGF at t=0 s. In the absence of cells, the signal does not change and stay below the noise level, defined as thrice the SD of the noise over the baseline. However, in the presence of 100,000 cells, an increase above this threshold (Figure 12A and C, $p<0.001$) in current is recorded above the noise level of the device 13.8 ± 5.0 s after the addition of VEGF. The reported delayed release of NO after VEGF stimulation agrees with previously published reports.[8,20,50]

The current increase in the presence of EA.hy926 was thus attributed to the activity of cells only, and more specifically to VEGF-stimulated NO release. The increase in amperometric current of 0.55 µA indicates that [NO]= 3.75 µM after exposure to VEGF, using the DEANONO-ate amperometric calibration. This high concentration is expected from the densely seeded EA.hy926 cells. Assuming that NO is stable for 10 s in oxygenated buffers, and considering there are 100,000 cells in a 2-µl sample, this corresponds to a NO production rate for a single cell of 4.5 10^6 molecules s^{-1}.

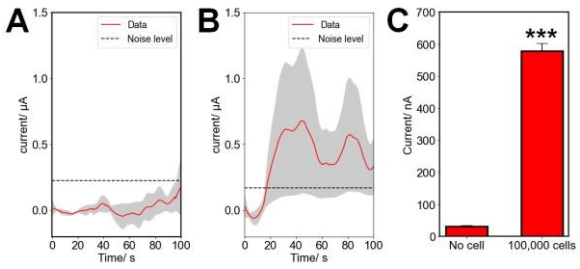

Figure 12: NO analysis in cultured cells on the paper chip. Average amperometric traces for A- no and B- 100,000 EA.hy926 cells maintained on the chips, stimulated at t=0 s with 20 ng.ml^{-1} VEGF, in PBS (for each case, n= 3 chips, mean±SD). C- Averages of the amperometric data (shown in A and B) recorded from 30 to 100 s for 0 and 100,000 cells maintained in the paper device, flowing VEGF stimulation (mean± SEM, n=3 for each case, Student's t-test ***: $p<0.001$)

5.5.7 Bioanalytical significance

For single endothelial or endocardial cells, [NO] following chemical or mechanical stimulation has been reported to be in the 100 nM to 1 µM range depending on the distance between the cell and the electrode, and the type of cell.[20,21,51] The instantaneous concentration of NO at the surface of

single endothelial cells was measured as ~ 1 μM for a sensed volume of 10^{-10} l,[51] which corresponds to a rate of release of NO of 6 10^6 molecules s^{-1} per cell, in agreement with our data. The discrepancies can be largely attributed to the difficulties in measuring the sensed volume, but this preliminary data nevertheless supports the use of paper NO sensor for the study of endothelial NO release.

Endothelial cells are typically used *in vitro* to grow artificial vasculature,[52] owing to their capability to form microvessels in response to angiogenic factors, like VEGF. This is not the case in the present assay, as the cells are tested a few hours after seeding. The fluorescence imaging clearly shows that the EA.hy926 are maintained as individual cells or in small clusters, not in large tubules. The assay is nevertheless significant as it provides quantitative information on the early steps of angiogenesis. Indeed, a preliminary angiogenic event is the release of NO which promotes endothelial cell motility and proliferation, and measuring this response of significance to highlight the angiogenic role of compounds and growth factors, even in individual cells or monolayers.[53–55] The VEGF concentration used here is also in agreement with the ones used for *in vitro* or *in vivo* assays.[7,53,56–58]

Finally, the cells are kept in a 3D matrix thanks to the capillary properties of paper, which increases the biomimicry of the assay. The use of porous paper as a device substrate allows for rapidly and easily building a 3D cell construct and to sense NO release in a 2 μl sample, thus providing easy access to quantitative measurements in an artificial tissue.[38]

5.6 Conclusion

NO paper-based sensors were fabricated and tested. Their selectivity against nitrite was tested, confirming their suitability for NO sensing. In comparison to carbon electrodes, the use of paper decreases the analytical properties of the sensor but provides an easy-to-use platform. Furthermore, the sensor characteristics were found to be suitable for multicellular applications. Importantly, their applicability to cell measurements was investigated, and time dynamics of NO release following VEGF exposure were successfully resolved. This supports the validity of using paper devices for investigating NO biology in 3D cell models.

5.7 Data availability

The data supporting this article have been included in the tables and figures.

5.8 Conflicts of interest

There are no conflicts to declare.

5.9 Author contributions

Conceptualization, R.T., methodology S.H.A., R.T., investigation, S.H.A., formal analysis, S.H.A., data curation S.H.A., validation, R.T., writing – original draft, S.H.A., R.T., writing – review and editing, S.H.A., R.T., supervision, R.T. All authors have read and agreed to the published version of the manuscript.

5.10 Acknowledgements

The FRQNT, NSERC, NFRF, Polytechnique Montréal and the TransMedTech Institute are gratefully acknowledged for funding.

5.11 References

[1] K.-D. Kröncke, K. Fehsel, V. Kolb-Bachofen, *Nitric Oxide* **1997**, *1*, 107–120.

[2] S. Korde Choudhari, M. Chaudhary, S. Bagde, A. R. Gadbail, V. Joshi, *World J. Surg. Oncol.* **2013**, *11*, 118.

[3] J. R. Klinger, P. J. Kadowitz, *Am. J. Cardiol.* **2017**, *120*, S71–S79.

[4] S. Moncada, E. A. Higgs, *Br. J. Pharmacol.* **2006**, *147*, S193–S201.

[5] R. M. J. Palmer, A. G. Ferrige, S. Moncada, *Nature* **1987**, *327*, 524–526.

[6] R. Trouillon, E. D. Williamson, R. J. Saint, D. O'Hare, *Biosens. Bioelectron.* **2012**, *38*, 138–144.

[7] A. Papapetropoulos, G. García-Cardeña, J. A. Madri, W. C. Sessa, *J. Clin. Invest.* **1997**, *100*, 3131–3139.

[8] R. Trouillon, D.-K. Kang, H. Park, S.-I. Chang, D. O'Hare, *Biochemistry* **2010**, *49*, 3282–3288.

[9] Y. Nakamura, H. Yasuoka, M. Tsujimoto, K. Yoshidome, M. Nakahara, K. Nakao, M. Nakamura, K. Kakudo, *Clin. Cancer Res.* **2006**, *12*, 1201–1207.

[10] P. Carmeliet, R. K. Jain, *Nature* **2000**, *407*, 249–257.

[11] H. T. Nguyen, L. N. Dupont, E. A. Cuttaz, A. M. Jean, R. Trouillon, M. A. M. Gijs, *Microelectron. Eng.* **2018**, *189*, 33–38.

[12] K. L. Meadows, H. I. Hurwitz, *Cold Spring Harb. Perspect. Med.* **2012**, *2*, DOI 10.1101/cshperspect.a006577.

[13] D. D. Thomas, X. Liu, S. P. Kantrow, J. R. Lancaster, *Proc. Natl. Acad. Sci.* **2001**, *98*, 355–360.

[14] J. Sun, X. Zhang, M. Broderick, H. Fein, *Sensors* **2003**, *3*, 276–284.

[15] H. Kojima, N. Nakatsubo, K. Kikuchi, S. Kawahara, Y. Kirino, H. Nagoshi, Y. Hirata, T. Nagano, *Anal. Chem.* **1998**, *70*, 2446–2453.

[16] X. Zhang, W.-S. Kim, N. Hatcher, K. Potgieter, L. L. Moroz, R. Gillette, J. V. Sweedler, *J. Biol. Chem.* **2002**, *277*, 48472–48478.

[17] M. D. Brown, M. H. Schoenfisch, *Chem. Rev.* **2019**, *119*, 11551–11575.

[18] A. J. Bard, L. R. Faulkner, *Electrochemical Methods: Fundamentals and Applications*, Wiley, New York, **2001**.

[19] L. Simonsson, M. E. Kurczy, R. Trouillon, F. Hook, A.-S. Cans, *Sci. Rep.* **2012**, *2*, 824.

[20] T. Malinski, Z. Taha, *Nature* **1992**, *358*, 676–678.

[21] V. Brovkovych, E. Stolarczyk, J. Oman, P. Tomboulian, T. Malinski, *J. Pharm. Biomed. Anal.* **1999**, *19*, 135–143.

[22] B. A. Patel, M. Arundell, K. H. Parker, M. S. Yeoman, D. O'Hare, *Anal. Chem.* **2006**, *78*, 7643–7648.

[23] T. Akyazi, L. Basabe-Desmonts, F. Benito-Lopez, *Anal. Chim. Acta* **2018**, *1001*, 1–17.

[24] D. A. Bruzewicz, M. Reches, G. M. Whitesides, *Anal. Chem.* **2008**, *80*, 3387–3392.

[25] E. Carrilho, A. W. Martinez, G. M. Whitesides, *Anal. Chem.* **2009**, *81*, 7091–7095.

[26] A. W. Martinez, S. T. Phillips, M. J. Butte, G. M. Whitesides, *Angew. Chem. Int. Ed.* **2007**, *46*, 1318–1320.

[27] A. W. Martinez, S. T. Phillips, G. M. Whitesides, E. Carrilho, *Anal. Chem.* **2010**, *82*, 3–10.

[28] B. Deka, R. Kalita, D. Bhatia, A. Mishra, *Sens. Int.* **2020**, *1*, 100004.

[29] W. Chen, X. Fang, H. Li, H. Cao, J. Kong, *Sci. Rep.* **2016**, *6*, 1–7.

[30] Z. Yao, P. Coatsworth, X. Shi, J. Zhi, L. Hu, R. Yan, F. Güder, H.-D. Yu, *Sens. Diagn.* **2022**, *1*, 312–342.

[31] J. Pelletier, R. Trouillon, *Electrochimica Acta* **2024**, *475*, 143528.

[32] R. Trouillon, M. A. M. Gijs, *ChemPhysChem* **2018**, *19*, 1164–1172.

[33] W. Dungchai, O. Chailapakul, C. S. Henry, *Anal. Chem.* **2009**, *81*, 5821–5826.

[34] J. Mettakoonpitak, K. Boehle, S. Nantaphol, P. Teengam, J. A. Adkins, M. Srisa-Art, C. S. Henry, *Electroanalysis* **2016**, *28*, 1420–1436.

[35] L. Bezinge, N. Tappauf, D. A. Richards, C.-J. Shih, A. J. deMello, *ACS Sens.* **2023**, *8*, 3964–3972.

[36] E. Noviana, C. S. Henry, *Curr. Opin. Electrochem.* **2020**, *23*, 1–6.

[37] A. T. Singh, D. Lantigua, A. Meka, S. Taing, M. Pandher, G. Camci-Unal, *Sensors* **2018**, *18*, 2838.

[38] R. Trouillon, M. A. M. Gijs, *Biosens. Bioelectron. X* **2023**, *14*, 100327.

[39] R. Derda, A. Laromaine, A. Mammoto, S. K. Y. Tang, T. Mammoto, D. E. Ingber, G. M. Whitesides, *Proc. Natl. Acad. Sci.* **2009**, *106*, 18457–18462.

[40] F. F. Tao, X. Xiao, K. F. Lei, I.-C. Lee, *BioChip J.* **2015**, *9*, 97–104.

[41] K. Ng, B. Gao, K. W. Yong, Y. Li, M. Shi, X. Zhao, Z. Li, X. Zhang, B. Pingguan-Murphy, H. Yang, F. Xu, *Mater. Today* **2017**, *20*, 32–44.

[42] R. Trouillon, M. A. M. Gijs, *RSC Adv.* **2016**, *6*, 31069–31073.

[43] R. Trouillon, M. C. Letizia, K. J. Menzies, L. Mouchiroud, J. Auwerx, K. Schoonjans, M. A. M. Gijs, *Integr. Biol.* **2017**, *9*, 810–819.

[44] S. Kasetsirikul, K. Clack, M. J. A. Shiddiky, N.-T. Nguyen, *Micromachines* **2022**, *13*, 48.

[45] Y. S. Kim, Y. Yang, C. S. Henry, *Sens. Actuators B Chem.* **2018**, *255*, 3654–3661.

[46] S. Griveau, C. Dumézy, P. Goldner, F. Bedioui, *Electrochem. Commun.* **2007**, *9*, 2551–2556.

[47] J. S. Mackie, P. Meares, E. K. Rideal, *Proc. R. Soc. Lond. Ser. Math. Phys. Sci.* **1955**, *232*, 498–509.

[48] R. Trouillon, A. G. Ewing, *Anal. Chem.* **2013**, *85*, 4822–4828.

[49] M. K. Priya, G. Sahu, D. R. Soto-Pantoja, N. Goldy, A. M. Sundaresan, V. Jadhav, T. R. Barathkumar, U. Saran, B. M. Jaffar Ali, D. D. Roberts, A. K. Bera, S. Chatterjee, *Angiogenesis* **2015**, *18*, 175–189.

[50] D. Feliers, X. Chen, N. Akis, G. G. Choudhury, M. Madaio, B. S. Kasinath, *Kidney Int.* **2005**, *68*, 1648–1659.

[51] D. J. Pinsky, S. Patton, S. Mesaros, V. Brovkovych, E. Kubaszewski, S. Grunfeld, T. Malinski, *Circ. Res.* **1997**, *81*, 372–379.

[52] S. Kim, H. Lee, M. Chung, N. L. Jeon, *Lab. Chip* **2013**, *13*, 1489–1500.

[53] R. Trouillon, C. Cheung, B. A. Patel, D. O'Hare, *Biochim. Biophys. Acta BBA-Gen. Subj.* **2010**, *1800*, 929–936.

[54] R. Trouillon, D.-K. Kang, S.-I. Chang, D. O'Hare, *Chem. Commun.* **2011**, *47*, 3421–3423.

[55] R. Trouillon, D.-K. Kang, S.-I. Chang, D. O'Hare, *Int. J. Mol. Sci.* **2022**, *23*, 15277.

[56] Y. Cao, P. Linden, J. Farnebo, R. Cao, A. Eriksson, V. Kumar, J.-H. Qi, L. Claesson-Welsh, K. Alitalo, *Proc. Natl. Acad. Sci.* **1998**, *95*, 14389–14394.

[57] D. Fukumura, T. Gohongi, A. Kadambi, Y. Izumi, J. Ang, C.-O. Yun, D. G. Buerk, P. L. Huang, R. K. Jain, *Proc. Natl. Acad. Sci.* **2001**, *98*, 2604–2609.

[58] S. A. Stacker, M. M. Halford, S. Roufail, C. Caesar, M. G. Achen, *J. Vis. Exp. JoVE* **2016**, 53867.

CHAPTER 6 DISCUSSION

The goal of this study was to fabricate paper sensors that could be used for the detection and quantification of NO. Secondary objectives of this study were to characterize paper sensors with electrochemistry as well as to determine the relations between current and NO concentration. Secondary objectives also included optimizing the sensitivity, LOD, and selectivity as well as determining the concentration of NO in cell culture after the injection of VEGF.

6.1 Relevance of the Study

NO is a biological molecule that performs a variety of roles in the human body. It carries out important functions in central nervous system (CNS), immune system, and the endothelial system. NO plays a central role in the vasculature. The release of NO is stimulated by pro-angiogenic growth factors such as VEGF. Angiogenesis refers to the development of new blood vessels that compose the vasculature. This is an essential process for all living things to grow beyond a minuscule size because the vasculature provides oxygen and nutrients necessary to sustain cell life. However, pathological angiogenesis, which involves the secretion of high concentrations of pro-angiogenic factors, is associated with cancer. As a result, the detection of NO can help indicate the presence of cancerous tumours. The early detection of cancer can be a matter of critical importance because of the greater efficacy of treatment methods in the beginning stages of the disease. The detection of NO is a challenging task because it is a radical molecule. Therefore, it is highly reactive with a short half-life and limited bioavailability. Many existing methods for NO detection are expensive, impractical, or lack the desired sensitivity, selectivity, and LOD for NO detection in humans. Electrochemical methods are the optimal tools for the detection of NO because of the easy ability of NO to be reduced and oxidized.

In this study, paper was utilized as a substrate for the detection of NO. Paper is an ideal material for a biomedical sensor because it is ubiquitous, inexpensive, and easy to use. Furthermore, paper sensors are biological and can be used to construct microfluidic channels. In addition, the surface of paper can be easily modified with simple techniques to improve the sensitivity, selectivity, and LOD of the paper-based sensor. The sensors produced in this study have a high sensitivity and a low LOD. They are also highly selective against molecules such as serotonin, ascorbic acid, and nitrite that could potentially interfere with the signal acquired from the NO.

Alternative methods of NO detection including fluorescence and colorimetric techniques such as the Greiss assay are limited in their sensitivity and selectivity as well as their ability to provide localized measurements *in vivo* or *in vitro*. This makes electrochemical methods crucial for detection and quantification of NO. The type of electrochemical sensor utilized for the detection of NO is also a critical matter because the current develops on the surface of the sensor.

The current state of the art NO electrochemical sensors are carbon fiber microelectrodes that have a detection limit on the nanomolar scale and can therefore detect physiologically relevant concentrations of NO *in vivo*. The paper sensors fabricated in this study can not perform this task as their detection limit is on the micromolar level. However, carbon fiber microelectrodes are more expensive to produce and more difficult to use as they are extremely fragile and break easily. Therefore, the low cost and ease of use of paper sensors mean that they remain desirable options for biomedical research and detection of NO *in vitro*. Furthermore, the research on paper sensors remains in its preliminary stages with the opportunity to improve the detection limit in future research that will be discussed in the subsequent chapter.

6.2 Applicability to Cell Measurements in Culture

One of the many advantages of paper-based sensors is that paper is biocompatible and therefore can be used in biological environments. The early results of this study demonstrate great promise in utilizing paper-based sensors for NO detection *in vitro*. The preliminary results show an increase in current measured by the sensors after the injection of VEGF using amperometry or DPV. This suggests that the paper sensors can be effective in the detection of NO in biological samples. However, further research is required to optimize the application of these sensors for both the *in vitro* and *in vivo* detection of NO.

CHAPTER 7 CONCLUSION AND RECOMMENDATIONS

The conclusion of this study is that NO sensors were fabricated from paper sensors that have been demonstrated to possess high sensitivity and selectivity and a relatively low LOD. They can also be utilized in biological environments and were successfully employed *in vitro* in cell culture to detect the change in concentration of NO before and after the injection of VEGF. While the LOD of the paper sensors fabricated in this study is not sufficiently low for the *in vivo* detection of NO in humans, the paper sensors have shown the ability to detect a rise of NO concentrations following the injection of VEGF, a growth factor that stimulates the release of NO.

7.1 Future Studies

Future research should focus on improving the sensitivity and LOD of the paper sensors. At the current moment, the LOD of paper sensors is on the micromolar scale and is insufficient for the detection of NO *in vivo* which exists at the nanomolar level (0.1-5nM). The sensitivity and LOD of the paper sensors can be improved through the deposition of additional layers of CNT ink to improve the conductivity of the sensors or through the deposition of a more highly conductive ink. As well, the sensitivity and the LOD can also be improved by reducing the size of the working part of the electrode which will likely produce a sharper current response.

The utilization of the sensors in the presence of tumour cells should also be explored in future studies. Tumour cells lead to higher NO concentration because of the pathological angiogenesis of cancerous cells, as mediated by angiogenic growth factors. The paper sensors could be used in the presence of tumour cells to compare the results between healthy and cancerous cells. This should then be repeated in the presence of various drugs inhibiting cancer angiogenesis which could potentially indicate the efficacy of these medications. This is because if the NO concentration in tumorous cell culture in the presence of medication decreases to the low levels in physiologically healthy levels, this suggests that the anti-tumour drugs are effective. This is one of many potential applications of the fabricated NO paper sensors in biomedical research. There are a variety of challenges that this research could face, specifically the potential interference from other biological molecules as well as the sensitivity of the sensors to the concentration of NO in medically relevant samples. It provides an opportunity to quantitatively benchmark different drugs and treatment strategies in clinical oncology or pharmacological research.

REFERENCES

[1] “Global Cancer Statistics 2020: GLOBOCAN Estimates of Incidence and Mortality Worldwide for 36 Cancers in 185 Countries - Sung - 2021 - CA: A Cancer Journal for Clinicians - Wiley Online Library.” Accessed: Jan. 24, 2024. [Online]. Available: https://acsjournals.onlinelibrary.wiley.com/doi/10.3322/caac.21660

[2] J. Noor, A. Chaudhry, R. Noor, and S. Batool, “Advancements and Applications of Liquid Biopsies in Oncology: A Narrative Review,” *Cureus*, vol. 15, no. 7, p. e42731, doi: 10.7759/cureus.42731.

[3] A. Pulumati, A. Pulumati, B. S. Dwarakanath, A. Verma, and R. V. L. Papineni, “Technological advancements in cancer diagnostics: Improvements and limitations,” *Cancer Rep.*, vol. 6, no. 2, Feb. 2023, doi: 10.1002/cnr2.1764.

[4] J. R. Hickok and D. D. Thomas, “Nitric Oxide and Cancer Therapy: The Emperor has NO Clothes,” *Curr. Pharm. Des.*, vol. 16, no. 4, pp. 381–391, 2010.

[5] B. A. Patel, M. Arundell, K. H. Parker, M. S. Yeoman, and D. O’Hare, “Detection of Nitric Oxide Release from Single Neurons in the Pond Snail, Lymnaea stagnalis,” *Anal. Chem.*, vol. 78, no. 22, pp. 7643–7648, Nov. 2006, doi: 10.1021/ac060863w.

[6] S. Moncada and E. A. Higgs, “The discovery of nitric oxide and its role in vascular biology,” *Br. J. Pharmacol.*, vol. 147, no. Suppl 1, pp. S193–S201, Jan. 2006, doi: 10.1038/sj.bjp.0706458.

[7] R. F. Furchgott, “Endothelium-Derived Relaxing Factor: Discovery, Early Studies, and Identifcation as Nitric Oxide (Nobel Lecture),” *Angew. Chem. Int. Ed Engl.*, vol. 38, no. 13–14, pp. 1870–1880, Jul. 1999, doi: 10.1002/(SICI)1521-3773(19990712)38:13/14<1870::AID-ANIE1870>3.0.CO;2-8.

[8] L. J. Ignarro, G. M. Buga, K. S. Wood, R. E. Byrns, and G. Chaudhuri, “Endothelium-derived relaxing factor produced and released from artery and vein is nitric oxide,” *Proc. Natl. Acad. Sci. U. S. A.*, vol. 84, no. 24, pp. 9265–9269, Dec. 1987, doi: 10.1073/pnas.84.24.9265.

[9] A. B. Levine, D. Punihaole, and T. B. Levine, “Characterization of the role of nitric oxide and its clinical applications,” *Cardiology*, vol. 122, no. 1, pp. 55–68, 2012, doi: 10.1159/000338150.

[10] K. Chen, R. N. Pittman, and A. S. Popel, “Nitric Oxide in the Vasculature: Where Does It Come From and Where Does It Go? A Quantitative Perspective,” *Antioxid. Redox Signal.*, vol. 10, no. 7, pp. 1185–1198, Jul. 2008, doi: 10.1089/ars.2007.1959.

[11] B. C. Kone, T. Kuncewicz, W. Zhang, and Z.-Y. Yu, “Protein interactions with nitric oxide synthases: controlling the right time, the right place, and the right amount of nitric oxide,” *Am. J. Physiol.-Ren. Physiol.*, vol. 285, no. 2, pp. F178–F190, Aug. 2003, doi: 10.1152/ajprenal.00048.2003.

[12] E. Goshi, G. Zhou, and Q. He, “Nitric oxide detection methods in vitro and in vivo,” *Med. Gas Res.*, vol. 9, no. 4, pp. 192–207, Dec. 2019, doi: 10.4103/2045-9912.273957.

[13] E. Nisoli and M. O. Carruba, “Nitric oxide and mitochondrial biogenesis,” *J. Cell Sci.*, vol. 119, no. Pt 14, pp. 2855–2862, Jul. 2006, doi: 10.1242/jcs.03062.

[14] M. Mitsuishi, K. Miyashita, and H. Itoh, “cGMP rescues mitochondrial dysfunction induced by glucose and insulin in myocytes,” *Biochem. Biophys. Res. Commun.*, vol. 367, no. 4, pp. 840–845, Mar. 2008, doi: 10.1016/j.bbrc.2008.01.017.

[15] R. D. Rakhit, M. H. Mojet, M. S. Marber, and M. R. Duchen, “Mitochondria as targets for nitric oxide-induced protection during simulated ischemia and reoxygenation in isolated neonatal cardiomyocytes,” *Circulation*, vol. 103, no. 21, pp. 2617–2623, May 2001, doi: 10.1161/01.cir.103.21.2617.

[16] W. J. Zenebe, R. R. Nazarewicz, M. S. Parihar, and P. Ghafourifar, “Hypoxia/Reoxygenation of Isolated Rat Heart Mitochondria Causes Cytochrome c Release and Oxidative Stress; Evidence for Involvement of Mitochondrial Nitric Oxide Synthase,” *J. Mol. Cell. Cardiol.*, vol. 43, no. 4, pp. 411–419, Oct. 2007, doi: 10.1016/j.yjmcc.2007.05.019.

[17] T. Münzel, R. Feil, A. Mülsch, S. M. Lohmann, F. Hofmann, and U. Walter, “Physiology and pathophysiology of vascular signaling controlled by guanosine 3’,5’-cyclic monophosphate-dependent protein kinase [corrected],” *Circulation*, vol. 108, no. 18, pp. 2172–2183, Nov. 2003, doi: 10.1161/01.CIR.0000094403.78467.C3.

[18] B. Lima, M. T. Forrester, D. T. Hess, and J. S. Stamler, “S-Nitrosylation in Cardiovascular Signaling,” *Circ. Res.*, vol. 106, no. 4, pp. 633–646, Mar. 2010, doi: 10.1161/CIRCRESAHA.109.207381.

[19] V. Calabrese, C. Mancuso, M. Calvani, E. Rizzarelli, D. A. Butterfield, and A. M. Giuffrida Stella, “Nitric oxide in the central nervous system: neuroprotection versus neurotoxicity,” *Nat. Rev. Neurosci.*, vol. 8, no. 10, pp. 766–775, Oct. 2007, doi: 10.1038/nrn2214.

[20] C. Hölscher and S. P. Rose, “An inhibitor of nitric oxide synthesis prevents memory formation in the chick,” *Neurosci. Lett.*, vol. 145, no. 2, pp. 165–167, Oct. 1992, doi: 10.1016/0304-3940(92)90012-v.

[21] G. A. Böhme *et al.*, “Altered synaptic plasticity and memory formation in nitric oxide synthase inhibitor-treated rats.,” *Proc. Natl. Acad. Sci. U. S. A.*, vol. 90, no. 19, pp. 9191–9194, Oct. 1993.

[22] N. E. Stagliano, W. D. Dietrich, R. Prado, E. J. Green, and R. Busto, “The role of nitric oxide in the pathophysiology of thromboembolic stroke in the rat,” *Brain Res.*, vol. 759, no. 1, pp. 32–40, Jun. 1997, doi: 10.1016/s0006-8993(97)00200-x.

[23] V. L. Dawson, T. M. Dawson, E. D. London, D. S. Bredt, and S. H. Snyder, “Nitric oxide mediates glutamate neurotoxicity in primary cortical cultures.,” *Proc. Natl. Acad. Sci. U. S. A.*, vol. 88, no. 14, pp. 6368–6371, Jul. 1991.

[24] C. Nathan, “Nitric oxide as a secretory product of mammalian cells,” *FASEB J. Off. Publ. Fed. Am. Soc. Exp. Biol.*, vol. 6, no. 12, pp. 3051–3064, Sep. 1992.

[25] S. Luckhart, Y. Vodovotz, L. Cui, and R. Rosenberg, “The mosquito Anopheles stephensi limits malaria parasite development with inducible synthesis of nitric oxide,” *Proc. Natl. Acad. Sci. U. S. A.*, vol. 95, no. 10, pp. 5700–5705, May 1998, doi: 10.1073/pnas.95.10.5700.

[26] J. L. Jiménez, J. González-Nicolás, S. Alvarez, M. Fresno, and M. A. Muñoz-Fernández, “Regulation of human immunodeficiency virus type 1 replication in human T lymphocytes by nitric oxide,” *J. Virol.*, vol. 75, no. 10, pp. 4655–4663, May 2001, doi: 10.1128/JVI.75.10.4655-4663.2001.

[27] R. M. J. Palmer, A. G. Ferrige, and S. Moncada, “Nitric oxide release accounts for the biological activity of endothelium-derived relaxing factor,” *Nature*, vol. 327, no. 6122, pp. 524–526, Jun. 1987, doi: 10.1038/327524a0.

[28] R. M. J. Palmer, D. S. Ashton, and S. Moncada, “Vascular endothelial cells synthesize nitric oxide from L-arginine,” *Nature*, vol. 333, no. 6174, pp. 664–666, Jun. 1988, doi: 10.1038/333664a0.

[29] D. Fukumura *et al.*, “Predominant role of endothelial nitric oxide synthase in vascular endothelial growth factor-induced angiogenesis and vascular permeability,” *Proc. Natl. Acad. Sci. U. S. A.*, vol. 98, no. 5, pp. 2604–2609, Feb. 2001, doi: 10.1073/pnas.041359198.

[30] “Nitric oxide regulation of microvascular oxygen exchange during hypoxia and hyperoxia.” Accessed: Jan. 15, 2024. [Online]. Available: https://journals.physiology.org/doi/epdf/10.1152/japplphysiol.01105.2005

[31] G. M. Buga, M. E. Gold, J. M. Fukuto, and L. J. Ignarro, “Shear stress-induced release of nitric oxide from endothelial cells grown on beads,” *Hypertens. Dallas Tex 1979*, vol. 17, no. 2, pp. 187–193, Feb. 1991, doi: 10.1161/01.hyp.17.2.187.

[32] N. M. Tsoukias, M. Kavdia, and A. S. Popel, “A theoretical model of nitric oxide transport in arterioles: frequency- vs. amplitude-dependent control of cGMP formation,” *Am. J. Physiol.-Heart Circ. Physiol.*, vol. 286, no. 3, pp. H1043–H1056, Mar. 2004, doi: 10.1152/ajpheart.00525.2003.

[33] P. Vallance, J. Collier, and S. Moncada, “Nitric oxide synthesised from L-arginine mediates endothelium dependent dilatation in human veins in vivo,” *Cardiovasc. Res.*, vol. 23, no. 12, pp. 1053–1057, Dec. 1989, doi: 10.1093/cvr/23.12.1053.

[34] W. G. Haynes, J. P. Noon, B. R. Walker, and D. J. Webb, “Inhibition of nitric oxide synthesis increases blood pressure in healthy humans,” *J. Hypertens.*, vol. 11, no. 12, pp. 1375–1380, Dec. 1993, doi: 10.1097/00004872-199312000-00009.

[35] P. L. Huang *et al.*, “Hypertension in mice lacking the gene for endothelial nitric oxide synthase,” *Nature*, vol. 377, no. 6546, pp. 239–242, Sep. 1995, doi: 10.1038/377239a0.

[36] R. De Caterina *et al.*, “Nitric oxide decreases cytokine-induced endothelial activation. Nitric oxide selectively reduces endothelial expression of adhesion molecules and proinflammatory cytokines.,” *J. Clin. Invest.*, vol. 96, no. 1, pp. 60–68, Jul. 1995.

[37] U. C. Garg and A. Hassid, “Nitric oxide-generating vasodilators and 8-bromo-cyclic guanosine monophosphate inhibit mitogenesis and proliferation of cultured rat vascular smooth muscle cells.,” *J. Clin. Invest.*, vol. 83, no. 5, pp. 1774–1777, May 1989.

[38] R. Sarkar, E. G. Meinberg, J. C. Stanley, D. Gordon, and R. C. Webb, “Nitric oxide reversibly inhibits the migration of cultured vascular smooth muscle cells,” *Circ. Res.*, vol. 78, no. 2, pp. 225–230, Feb. 1996, doi: 10.1161/01.res.78.2.225.

[39] J. S. Lee, C. Adrie, H. J. Jacob, J. D. Roberts, W. M. Zapol, and K. D. Bloch, “Chronic inhalation of nitric oxide inhibits neointimal formation after balloon-induced arterial injury,” *Circ. Res.*, vol. 78, no. 2, pp. 337–342, Feb. 1996, doi: 10.1161/01.res.78.2.337.

[40] H. Matsushita, E. Chang, A. J. Glassford, J. P. Cooke, C.-P. Chiu, and P. S. Tsao, “eNOS Activity Is Reduced in Senescent Human Endothelial Cells,” *Circ. Res.*, vol. 89, no. 9, pp. 793–798, Oct. 2001, doi: 10.1161/hh2101.098443.

[41] S. R. Kashyap *et al.*, “Insulin Resistance Is Associated with Impaired Nitric Oxide Synthase Activity in Skeletal Muscle of Type 2 Diabetic Subjects,” *J. Clin. Endocrinol. Metab.*, vol. 90, no. 2, pp. 1100–1105, Feb. 2005, doi: 10.1210/jc.2004-0745.

[42] A. C. Curnow *et al.*, “Low Nitric Oxide Bioavailability Increases Renin Production in the Collecting Duct,” *Front. Physiol.*, vol. 11, p. 559341, 2020, doi: 10.3389/fphys.2020.559341.

[43] J. Chen *et al.*, “Nitric oxide bioavailability dysfunction involves in atherosclerosis,” *Biomed. Pharmacother.*, vol. 97, pp. 423–428, Jan. 2018, doi: 10.1016/j.biopha.2017.10.122.

[44] D. Yao, A. Vlessidis, and N. Evmiridis, “Determination of Nitric Oxide in Biological Samples,” *Microchim. Acta*, vol. 147, pp. 1–20, Jun. 2004, doi: 10.1007/s00604-004-0212-8.

[45] C. N. Hall and J. Garthwaite, “What is the real physiological NO concentration in vivo?,” *Nitric Oxide*, vol. 21, no. 2, pp. 92–103, Sep. 2009, doi: 10.1016/j.niox.2009.07.002.

[46] D. Tsikas, “Analysis of nitrite and nitrate in biological fluids by assays based on the Griess reaction: appraisal of the Griess reaction in the L-arginine/nitric oxide area of research,” *J.*

Chromatogr. B Analyt. Technol. Biomed. Life. Sci., vol. 851, no. 1–2, pp. 51–70, May 2007, doi: 10.1016/j.jchromb.2006.07.054.

[47] L. Schmölz, M. Wallert, and S. Lorkowski, "Optimized incubation regime for nitric oxide measurements in murine macrophages using the Griess assay," *J. Immunol. Methods*, vol. 449, pp. 68–70, Oct. 2017, doi: 10.1016/j.jim.2017.06.012.

[48] R. V Pinto, F. Antunes, J. Pires, A. Silva-Herdade, and M. L. Pinto, "A Comparison of Different Approaches to Quantify Nitric Oxide Release from NO-Releasing Materials in Relevant Biological Media," *Mol. Basel Switz.*, vol. 25, no. 11, p. 2580, Jun. 2020, doi: 10.3390/molecules25112580.

[49] A. Gomes, E. Fernandes, and J. L. F. C. Lima, "Use of fluorescence probes for detection of reactive nitrogen species: a review," *J. Fluoresc.*, vol. 16, no. 1, pp. 119–139, Jan. 2006, doi: 10.1007/s10895-005-0030-3.

[50] H. Kojima *et al.*, "Detection and Imaging of Nitric Oxide with Novel Fluorescent Indicators: Diaminofluoresceins," *Anal. Chem.*, vol. 70, no. 13, pp. 2446–2453, Jul. 1998, doi: 10.1021/ac9801723.

[51] M. G. Espey, K. M. Miranda, D. D. Thomas, and D. A. Wink, "Ingress and reactive chemistry of nitroxyl-derived species within human cells," *Free Radic. Biol. Med.*, vol. 33, no. 6, pp. 827–834, Sep. 2002, doi: 10.1016/S0891-5849(02)00978-4.

[52] R. Radi, T. P. Cosgrove, J. S. Beckman, and B. A. Freeman, "Peroxynitrite-induced luminol chemiluminescence.," *Biochem. J.*, vol. 290, no. Pt 1, pp. 51–57, Feb. 1993.

[53] D. Tsikas *et al.*, "Assessment of nitric oxide synthase activity in vitro and in vivo by gas chromatography–mass spectrometry," *J. Chromatogr. B. Biomed. Sci. App.*, vol. 742, no. 1, pp. 143–153, May 2000, doi: 10.1016/S0378-4347(00)00142-0.

[54] D. Tsikas, "Simultaneous Derivatization and Quantification of the Nitric Oxide Metabolites Nitrite and Nitrate in Biological Fluids by Gas Chromatography/Mass Spectrometry," *Anal. Chem.*, vol. 72, no. 17, pp. 4064–4072, Sep. 2000, doi: 10.1021/ac9913255.

[55] A. Ciszewski and G. Milczarek, "Electrochemical detection of nitric oxide using polymer modified electrodes," *Talanta*, vol. 61, no. 1, pp. 11–26, Sep. 2003, doi: 10.1016/S0039-9140(03)00355-2.

[56] K. Ichimori, H. Ishida, M. Fukahori, H. Nakazawa, and E. Murakami, “Practical nitric oxide measurement employing a nitric oxide-selective electrode,” *Rev. Sci. Instrum.*, vol. 65, no. 8, pp. 2714–2718, Aug. 1994, doi: 10.1063/1.1144674.

[57] K. Shibuki, “An electrochemical microprobe for detecting nitric oxide release in brain tissue,” *Neurosci. Res.*, vol. 9, no. 1, pp. 69–76, Sep. 1990, doi: 10.1016/0168-0102(90)90048-J.

[58] F. Bedioui, S. Trevin, and J. Devynck, “The use of gold electrodes in the electrochemical detection of nitric oxide in aqueous solution,” *J. Electroanal. Chem.*, vol. 377, no. 1, pp. 295–298, Oct. 1994, doi: 10.1016/0022-0728(94)03642-X.

[59] B. W. Allen and C. A. Piantadosi, “Electrochemical activation of electrodes for amperometric detection of nitric oxide,” *Nitric Oxide*, vol. 8, no. 4, pp. 243–252, Jun. 2003, doi: 10.1016/S1089-8603(03)00029-6.

[60] T. Malinski and Z. Taha, “Nitric oxide release from a single cell measured in situ by a porphyrinic-based microsensor,” *Nature*, vol. 358, no. 6388, Art. no. 6388, Aug. 1992, doi: 10.1038/358676a0.

[61] E. M. Ahmed, “Hydrogel: Preparation, characterization, and applications: A review,” *J. Adv. Res.*, vol. 6, no. 2, pp. 105–121, Mar. 2015, doi: 10.1016/j.jare.2013.07.006.

[62] S. Bashir *et al.*, “Fundamental Concepts of Hydrogels: Synthesis, Properties, and Their Applications,” *Polymers*, vol. 12, no. 11, p. 2702, Nov. 2020, doi: 10.3390/polym12112702.

[63] E. Caló and V. V. Khutoryanskiy, “Biomedical applications of hydrogels: A review of patents and commercial products,” *Eur. Polym. J.*, vol. 65, pp. 252–267, Apr. 2015, doi: 10.1016/j.eurpolymj.2014.11.024.

[64] N. Hasan *et al.*, “Recent advancements of nitric oxide-releasing hydrogels for wound dressing applications,” *J. Pharm. Investig.*, vol. 53, no. 6, pp. 781–801, Nov. 2023, doi: 10.1007/s40005-023-00636-9.

[65] M. J. Malone-Povolny, S. E. Maloney, and M. H. Schoenfisch, “Nitric Oxide Therapy for Diabetic Wound Healing,” *Adv. Healthc. Mater.*, vol. 8, no. 12, p. e1801210, Jun. 2019, doi: 10.1002/adhm.201801210.

[66] E. M. Hetrick and M. H. Schoenfisch, “Reducing implant-related infections: active release strategies,” *Chem. Soc. Rev.*, vol. 35, no. 9, pp. 780–789, Aug. 2006, doi: 10.1039/B515219B.

[67] B. A. Aderibigbe, “Hybrid-Based Wound Dressings: Combination of Synthetic and Biopolymers,” *Polymers*, vol. 14, no. 18, p. 3806, Sep. 2022, doi: 10.3390/polym14183806.

[68] G. Zheng *et al.*, “Controllable release of nitric oxide from an injectable alginate hydrogel,” *Int. J. Biol. Macromol.*, vol. 252, p. 126371, Dec. 2023, doi: 10.1016/j.ijbiomac.2023.126371.

[69] G. Mummaleti and F. Kong, “Fabrication, properties and applications of xerogels in food processing,” *J. Agric. Food Res.*, vol. 11, p. 100506, Mar. 2023, doi: 10.1016/j.jafr.2023.100506.

[70] A. Meiller, E. Sequeira, and S. Marinesco, “Electrochemical Nitric Oxide Microsensors Based on a Fluorinated Xerogel Screening Layer for in Vivo Brain Monitoring,” *Anal. Chem.*, vol. 92, no. 2, pp. 1804–1810, Jan. 2020, doi: 10.1021/acs.analchem.9b03621.

[71] A. A. Khalil, U. ur Rahman, M. R. Khan, A. Sahar, T. Mehmood, and M. Khan, “Essential oil eugenol: sources, extraction techniques and nutraceutical perspectives,” *RSC Adv.*, vol. 7, no. 52, pp. 32669–32681, Jun. 2017, doi: 10.1039/C7RA04803C.

[72] “Eugenol (Clove Oil),” in *LiverTox: Clinical and Research Information on Drug-Induced Liver Injury*, Bethesda (MD): National Institute of Diabetes and Digestive and Kidney Diseases, 2012. Accessed: Feb. 29, 2024. [Online]. Available: http://www.ncbi.nlm.nih.gov/books/NBK551727/

[73] M. F. Nisar, M. Khadim, M. Rafiq, J. Chen, Y. Yang, and C. C. Wan, “Pharmacological Properties and Health Benefits of Eugenol: A Comprehensive Review,” *Oxid. Med. Cell. Longev.*, vol. 2021, p. 2497354, Aug. 2021, doi: 10.1155/2021/2497354.

[74] R. Li *et al.*, “A flexible and physically transient electrochemical sensor for real-time wireless nitric oxide monitoring,” *Nat. Commun.*, vol. 11, p. 3207, Jun. 2020, doi: 10.1038/s41467-020-17008-8.

[75] A. Ciszewski and G. Milczarek, “A New Nafion-Free Bipolymeric Sensor for Selective and Sensitive Detection of Nitric Oxide,” *Electroanalysis*, vol. 10, no. 11, pp. 791–793, 1998, doi: 10.1002/(SICI)1521-4109(199809)10:11<791::AID-ELAN791>3.0.CO;2-H.

[76] D. Quinton *et al.*, “On-chip multi-electrochemical sensor array platform for simultaneous screening of nitric oxide and peroxynitrite,” *Lab. Chip*, vol. 11, no. 7, pp. 1342–1350, Apr. 2011, doi: 10.1039/C0LC00585A.

[77] Z. Yao *et al.*, “Paper-based sensors for diagnostics, human activity monitoring, food safety and environmental detection,” *Sens. Diagn.*, vol. 1, no. 3, pp. 312–342, 2022, doi: 10.1039/D2SD00017B.

[78] W. J. Paschoalino *et al.*, “Emerging Considerations for the Future Development of Electrochemical Paper-Based Analytical Devices,” *ChemElectroChem*, vol. 6, no. 1, pp. 10–30, 2019, doi: 10.1002/celc.201800677.

[79] A. W. Martinez, S. T. Phillips, G. M. Whitesides, and E. Carrilho, “Diagnostics for the Developing World: Microfluidic Paper-Based Analytical Devices,” *Anal. Chem.*, vol. 82, no. 1, pp. 3–10, Jan. 2010, doi: 10.1021/ac9013989.

[80] R. Pelton, “Bioactive paper provides a low-cost platform for diagnostics,” *TrAC Trends Anal. Chem.*, vol. 28, no. 8, pp. 925–942, Sep. 2009, doi: 10.1016/j.trac.2009.05.005.

[81] A. W. Martinez, S. T. Phillips, M. J. Butte, and G. M. Whitesides, “Patterned Paper as a Platform for Inexpensive, Low Volume, Portable Bioassays,” *Angew. Chem. Int. Ed Engl.*, vol. 46, no. 8, pp. 1318–1320, 2007, doi: 10.1002/anie.200603817.

[82] D. A. Bruzewicz, M. Reches, and G. M. Whitesides, “Low-Cost Printing of Poly(dimethylsiloxane) Barriers To Define Microchannels in Paper,” *Anal. Chem.*, vol. 80, no. 9, pp. 3387–3392, May 2008, doi: 10.1021/ac702605a.

[83] A. W. Martinez, S. T. Phillips, E. Carrilho, S. W. I. Thomas, H. Sindi, and G. M. Whitesides, “Simple Telemedicine for Developing Regions: Camera Phones and Paper-Based Microfluidic Devices for Real-Time, Off-Site Diagnosis,” *Anal. Chem.*, vol. 80, no. 10, pp. 3699–3707, May 2008, doi: 10.1021/ac800112r.

[84] A. W. Martinez, S. T. Phillips, and G. M. Whitesides, “Three-dimensional microfluidic devices fabricated in layered paper and tape,” *Proc. Natl. Acad. Sci.*, vol. 105, no. 50, pp. 19606–19611, Dec. 2008, doi: 10.1073/pnas.0810903105.

[85] J. Adkins, K. Boehle, and C. Henry, “Electrochemical paper-based microfluidic devices,” *ELECTROPHORESIS*, vol. 36, no. 16, pp. 1811–1824, 2015, doi: 10.1002/elps.201500084.

[86] W. Dungchai, O. Chailapakul, and C. S. Henry, “Electrochemical Detection for Paper-Based Microfluidics,” *Anal. Chem.*, vol. 81, no. 14, pp. 5821–5826, Jul. 2009, doi: 10.1021/ac9007573.

[87] J. Mettakoonpitak, J. Volckens, and C. S. Henry, “Janus Electrochemical Paper-Based Analytical Devices for Metals Detection in Aerosol Samples,” *Anal. Chem.*, vol. 92, no. 1, pp. 1439–1446, Jan. 2020, doi: 10.1021/acs.analchem.9b04632.

[88] S. Nantaphol *et al.*, “Janus electrochemistry: Simultaneous electrochemical detection at multiple working conditions in a paper-based analytical device,” *Anal. Chim. Acta*, vol. 1056, pp. 88–95, May 2019, doi: 10.1016/j.aca.2019.01.026.

[89] Z. Nie, F. Deiss, X. Liu, O. Akbulut, and G. M. Whitesides, “Integration of paper-based microfluidic devices with commercial electrochemical readers,” *Lab. Chip*, vol. 10, no. 22, pp. 3163–3169, Oct. 2010, doi: 10.1039/C0LC00237B.

[90] C. Zhao, M. M. Thuo, and X. Liu, “A microfluidic paper-based electrochemical biosensor array for multiplexed detection of metabolic biomarkers,” *Sci. Technol. Adv. Mater.*, vol. 14, no. 5, p. 054402, Oct. 2013, doi: 10.1088/1468-6996/14/5/054402.

[91] X. Li, C. Zhao, and X. Liu, “A paper-based microfluidic biosensor integrating zinc oxide nanowires for electrochemical glucose detection,” *Microsyst. Nanoeng.*, vol. 1, no. 1, pp. 1–7, Aug. 2015, doi: 10.1038/micronano.2015.14.

[92] M. Su *et al.*, “Paper-based electrochemical cyto-device for sensitive detection of cancer cells and in situ anticancer drug screening,” *Anal. Chim. Acta*, vol. 847, pp. 1–9, Oct. 2014, doi: 10.1016/j.aca.2014.08.013.

[93] F. Liu, S. Ge, J. Yu, M. Yan, and X. Song, “Electrochemical device based on a Pt nanosphere-paper working electrode for in situ and real-time determination of the flux of H2O2 releasing from SK-BR-3 cancer cells,” *Chem. Commun.*, vol. 50, no. 71, pp. 10315–10318, Aug. 2014, doi: 10.1039/C4CC04199B.

[94] K. M. Yamada and E. Cukierman, “Modeling tissue morphogenesis and cancer in 3D,” *Cell*, vol. 130, no. 4, pp. 601–610, Aug. 2007, doi: 10.1016/j.cell.2007.08.006.

[95] F. Pampaloni, E. G. Reynaud, and E. H. K. Stelzer, “The third dimension bridges the gap between cell culture and live tissue,” *Nat. Rev. Mol. Cell Biol.*, vol. 8, no. 10, pp. 839–845, Oct. 2007, doi: 10.1038/nrm2236.

[96] R. Derda *et al.*, “Paper-supported 3D cell culture for tissue-based bioassays,” *Proc. Natl. Acad. Sci.*, vol. 106, no. 44, pp. 18457–18462, Nov. 2009, doi: 10.1073/pnas.0910666106.

[97] K. Ng *et al.*, “Paper-based cell culture platform and its emerging biomedical applications,” *Mater. Today*, vol. 20, no. 1, pp. 32–44, Jan. 2017, doi: 10.1016/j.mattod.2016.07.001.

[98] E. A. Jaffe, R. L. Nachman, C. G. Becker, and C. R. Minick, “Culture of Human Endothelial Cells Derived from Umbilical Veins. IDENTIFICATION BY MORPHOLOGIC AND IMMUNOLOGIC CRITERIA,” *J. Clin. Invest.*, vol. 52, no. 11, pp. 2745–2756, Nov. 1973.

[99] M. Targosz-Korecka, G. D. Brzezinka, K. E. Malek, E. Stępień, and M. Szymonski, “Stiffness memory of EA.hy926 endothelial cells in response to chronic hyperglycemia,” *Cardiovasc. Diabetol.*, vol. 12, no. 1, p. 96, Jun. 2013, doi: 10.1186/1475-2840-12-96.

[100] K. Ahn, S. Pan, K. Beningo, and D. Hupe, “A permanent human cell line (EA.hy926) preserves the characteristics of endothelin converting enzyme from primary human umbilical vein endothelial cells,” *Life Sci.*, vol. 56, no. 26, pp. 2331–2341, May 1995, doi: 10.1016/0024-3205(95)00227-W.

[101] E. R. Weibel and G. E. Palade, “NEW CYTOPLASMIC COMPONENTS IN ARTERIAL ENDOTHELIA,” *J. Cell Biol.*, vol. 23, no. 1, pp. 101–112, Oct. 1964.

[102] C. J. Edgell *et al.*, “Endothelium specific Weibel-Palade bodies in a continuous human cell line, EA.hy926,” *Vitro Cell. Dev. Biol. J. Tissue Cult. Assoc.*, vol. 26, no. 12, pp. 1167–1172, Dec. 1990, doi: 10.1007/BF02623694.

[103] R. L. Nachman and E. A. Jaffe, “Endothelial cell culture: beginnings of modern vascular biology,” *J. Clin. Invest.*, vol. 114, no. 8, pp. 1037–1040, Oct. 2004, doi: 10.1172/JCI200423284.

[104] J. Bauer *et al.*, “In vitro model of angiogenesis using a human endothelium-derived permanent cell line: contributions of induced gene expression, G-proteins, and integrins,” *J. Cell. Physiol.*, vol. 153, no. 3, pp. 437–449, Dec. 1992, doi: 10.1002/jcp.1041530302.

[105] T. L. Place, F. E. Domann, and A. J. Case, “Limitations of Oxygen Delivery to Cells in Culture: An Underappreciated Problem in Basic and Translational Research,” *Free Radic. Biol. Med.*, vol. 113, pp. 311–322, Dec. 2017, doi: 10.1016/j.freeradbiomed.2017.10.003.

[106] A. M. Duffy, D. J. Bouchier-Hayes, and J. H. Harmey, “Vascular Endothelial Growth Factor (VEGF) and Its Role in Non-Endothelial Cells: Autocrine Signalling by VEGF,” in *Madame Curie Bioscience Database [Internet]*, Landes Bioscience, 2013. Accessed: Mar. 18, 2024. [Online]. Available: https://www.ncbi.nlm.nih.gov/books/NBK6482/

[107] C. S. Melincovici *et al.*, “Vascular endothelial growth factor (VEGF) - key factor in normal and pathological angiogenesis,” *Romanian J. Morphol. Embryol. Rev. Roum. Morphol. Embryol.*, vol. 59, no. 2, pp. 455–467, 2018.

[108] J. P. Cooke and D. W. Losordo, “Nitric Oxide and Angiogenesis,” *Circulation*, vol. 105, no. 18, pp. 2133–2135, May 2002, doi: 10.1161/01.CIR.0000014928.45119.73.

[109] D. G. Duda, T. T. Batchelor, C. G. Willett, and R. K. Jain, “VEGF-targeted cancer therapy strategies: current progress, hurdles and future prospects,” *Trends Mol. Med.*, vol. 13, no. 6, pp. 223–230, Jun. 2007, doi: 10.1016/j.molmed.2007.04.001.

[110] P. Carmeliet and R. K. Jain, “Angiogenesis in cancer and other diseases,” *Nature*, vol. 407, no. 6801, pp. 249–257, Sep. 2000, doi: 10.1038/35025220.

[111] R. K. Jain, “Normalization of Tumor Vasculature: An Emerging Concept in Antiangiogenic Therapy,” *Science*, vol. 307, no. 5706, pp. 58–62, Jan. 2005, doi: 10.1126/science.1104819.

[112] S. Goel *et al.*, “NORMALIZATION OF THE VASCULATURE FOR TREATMENT OF CANCER AND OTHER DISEASES,” *Physiol. Rev.*, vol. 91, no. 3, pp. 1071–1121, Jul. 2011, doi: 10.1152/physrev.00038.2010.

[113] R. K. Jain, “Determinants of Tumor Blood Flow: A Review1,” *Cancer Res.*, vol. 48, no. 10, pp. 2641–2658, May 1988.

[114] L. Morbidelli, S. Donnini, and M. Ziche, “Chapter 4 - Therapeutic Implications of the Nitric Oxide Pathway in the Angiogenesis of Tumors and Inflammatory-Related Disorders,” in *Therapeutic Application of Nitric Oxide in Cancer and Inflammatory Disorders*, L. Morbidelli and B. Bonavida, Eds., Academic Press, 2019, pp. 65–91. doi: 10.1016/B978-0-12-816545-4.00004-9.

[115] A. Arulraj and S. T. Nishanthi, “Chapter 13 - 2D materials–based flexible supercapacitors for high energy storage devices,” in *Nanostructured, Functional, and Flexible Materials for Energy Conversion and Storage Systems*, A. Pandikumar and P. Rameshkumar, Eds., Elsevier, 2020, pp. 417–436. doi: 10.1016/B978-0-12-819552-9.00013-0.

[116] B. J. Venton and D. J. DiScenza, “Chapter 3 - Voltammetry,” in *Electrochemistry for Bioanalysis*, B. Patel, Ed., Elsevier, 2020, pp. 27–50. doi: 10.1016/B978-0-12-821203-5.00004-X.

[117] G. Greczynski and L. Hultman, “X-ray photoelectron spectroscopy: Towards reliable binding energy referencing,” *Prog. Mater. Sci.*, vol. 107, p. 100591, Jan. 2020, doi: 10.1016/j.pmatsci.2019.100591.

[118] V. Jain, M. C. Biesinger, and M. R. Linford, “The Gaussian-Lorentzian Sum, Product, and Convolution (Voigt) functions in the context of peak fitting X-ray photoelectron spectroscopy (XPS) narrow scans,” *Appl. Surf. Sci.*, vol. 447, pp. 548–553, Jul. 2018, doi: 10.1016/j.apsusc.2018.03.190.

[119] S. Griveau, C. Dumézy, P. Goldner, and F. Bedioui, “Electrochemical analysis of the kinetics of nitric oxide release from two diazeniumdiolates in buffered aqueous solutions,” *Electrochem. Commun.*, vol. 9, no. 10, pp. 2551–2556, Oct. 2007, doi: 10.1016/j.elecom.2007.07.037.

APPENDIX A SENSITIVITY AND LIMIT OF DETECTION

Table A.1 Electrode Sensitivities

Electrode Number	**Sensitivity/A.M^{-1}m^{-2}**
1	373.1875
2	360.4285714
3	752.8571429
4	488.3125
5	972.8571429
6	394.3571429
7	800.9166667
8	865
9	498.5
10	278
11	75.875
Median	488.3125
Quartile 1	366.8080357
Quartile 3	776.8869048

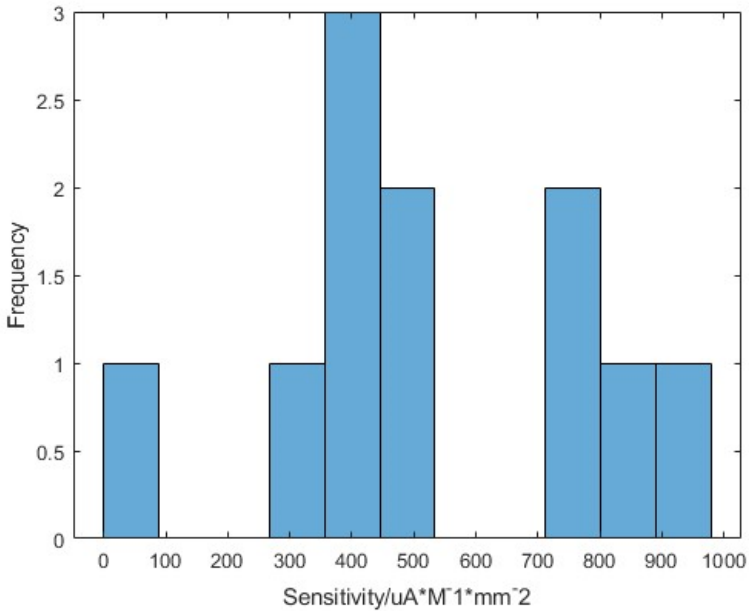

Figure A-1: Historgram of Electrode Sensitivities

Table A.2: Electrode Limits of Detection

Electrode	**LOD/uM**
1	1.76
2	1.53
3	1.27
4	2.88
5	4.52
6	2.39
7	3.77
8	3.40
9	2.77

10	0.726
11	1.10
Median	2.39
Quartile 1	1.40
Quartile 3	3.14

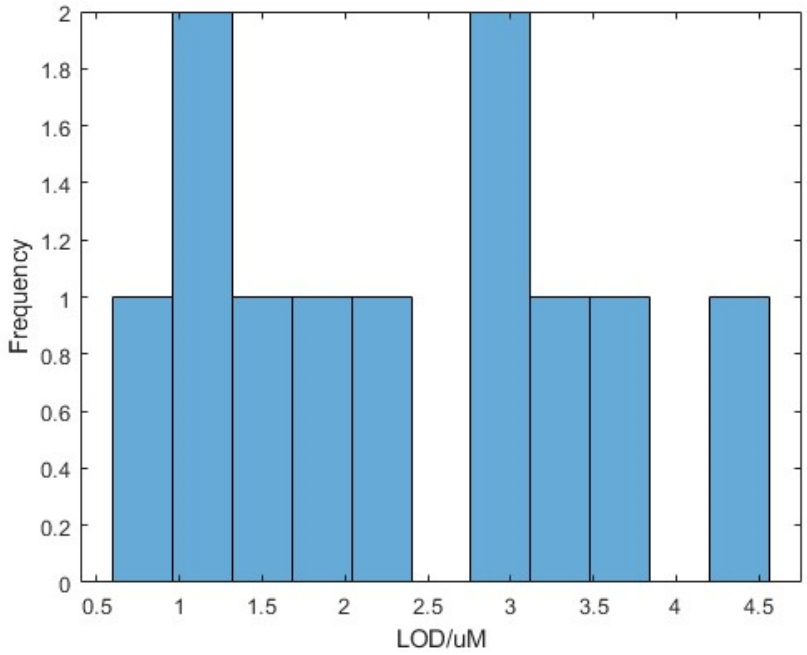

Figure A-2: Histogram of Electrode Limits of Detection

APPENDIX B CALCULATED NITRIC OXIDE RELEASE

The ODE defining the release of NO from an injection of NONOate solution as a function of time[119].

$$\frac{d[NO]}{dt} + k_2'[NO]^2 = k'e^{-k_1 t}$$

$$k_2' = 4k_2[O_2]$$

$$k_2 = 2 \times 10^6 M^{-2} s^{-1}$$

$$[O_2] = 1.3 \times 10^{-3} atm^{-1}$$

$$k' = v_{NO} k_1 [NONOate]_0$$

$$v_{NO} = 1.5$$

$$k_1 = 28.5 \times 10^{-4} s^{-1}$$

$$[NONOate]_0 = 100 \times 10^{-6} M$$

$$[NONOate]_0 = 200 \times 10^{-6} M$$

$$[NONOate]_0 = 300 \times 10^{-6} M$$

For 100uM of DEANONO-ate:

$$\frac{d[NO]}{dt} + 2.08 \times 10^3 [NO]^2 = 4.275 \times 10^{-7} e^{-28.5 \times 10^{-4} t}$$

For 200uM of DEANONO-ate:

$$\frac{d[NO]}{dt} + 2.08 \times 10^3 [NO]^2 = 8.55 \times 10^{-7} e^{-28.5 \times 10^{-4} t}$$

For 300uM of DEANONO-ate:

$$\frac{d[NO]}{dt} + 2.08 \times 10^3 [NO]^2 = 1.282 \times 10^{-6} e^{-28.5 \times 10^{-4} t}$$

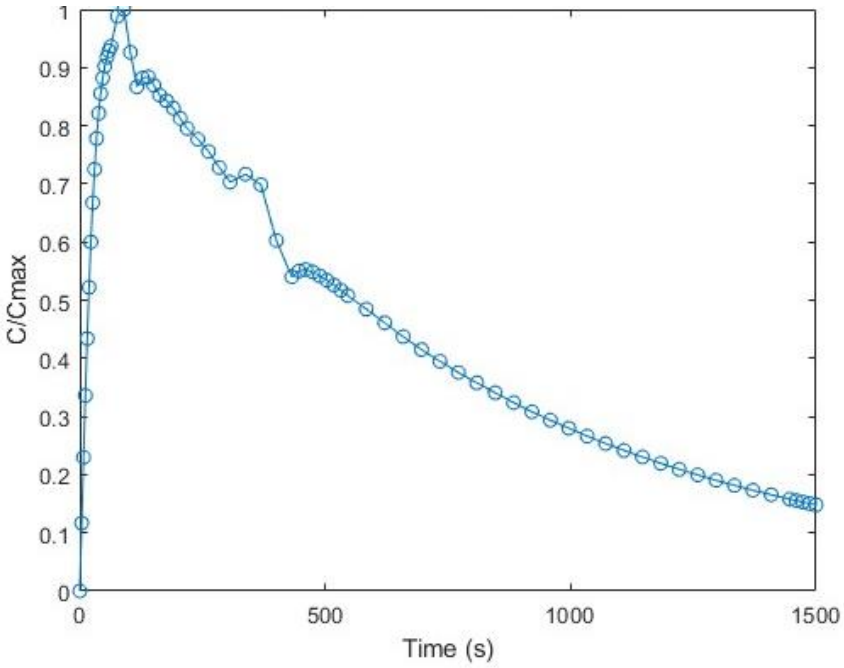

Figure B-3: ODE Solution for Nitric Oxide Release for 100uM DEANONO-ate Injection.

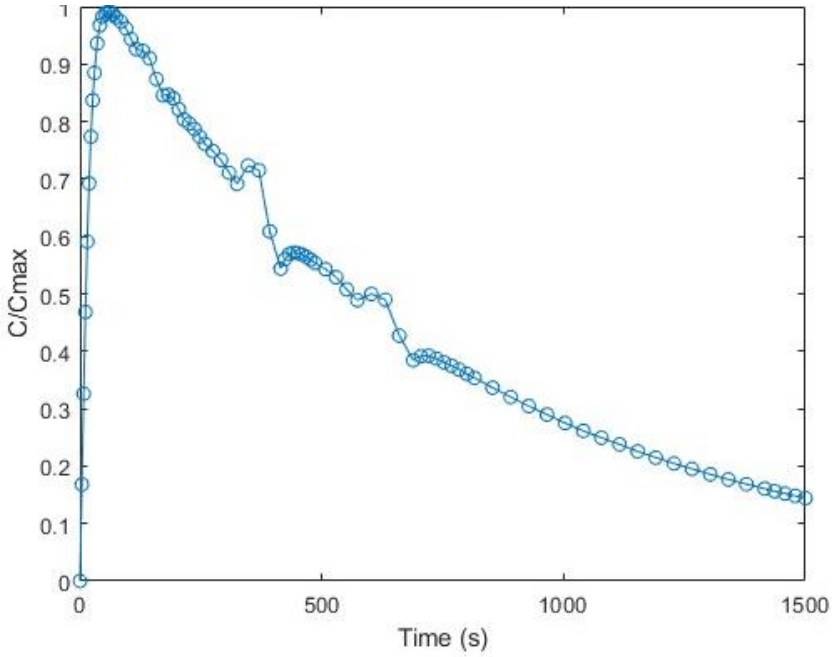

Figure B-4: ODE Solution for Nitric Oxide Release for 200uM DEANONO-ate Injection.

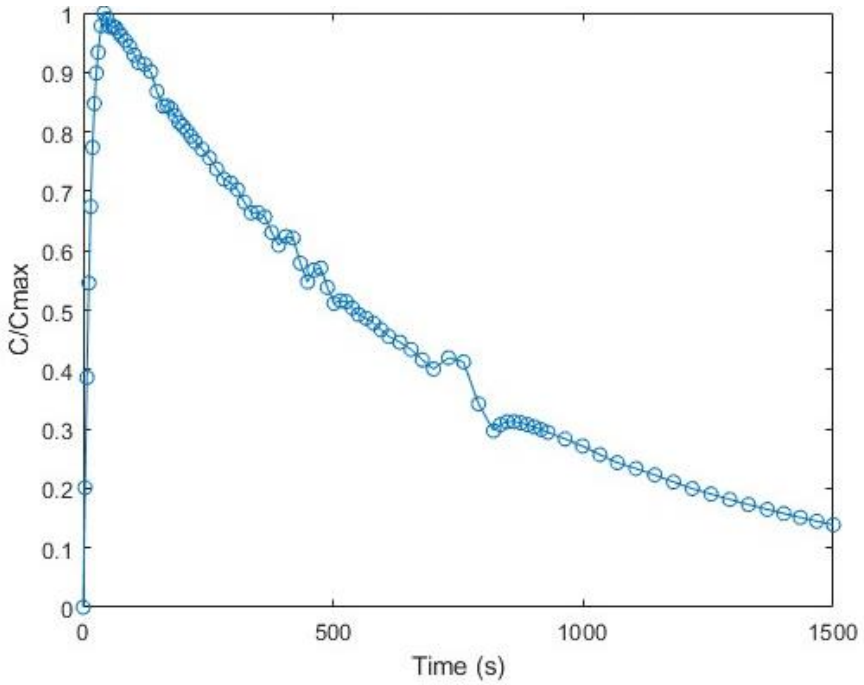

Figure B-5: ODE Solution for Nitric Oxide Release for 300uM DEANONO-ate Injection.

Table B-1: Time Required to Achieve Maximum Nitric Oxide Concentration and Value of the Concentration.

$[DEA\text{-}NONOate]_0$ (µM)	T_{max} (min)	Max [NO] (µM)
100	1.4974	13.576
200	0.9590	18.666
300	0.6938	23.461